UCL Université catholique de Louvain

École polytechnique de Louvain (EPL)

Rejection performance and stability of MF/UF ceramic membranes towards TiO_2 photocatalyst in PMRs

Dissertation presented by
Robin HAINAUT

for obtaining the Master's degree in
Chemical and Materials Engineering

Supervisor(s)
Prof. Patricia LUIS ALCONERO, Raphaël JANSSENS

Reader(s)
Prof. Denis MIGNON, Prof. Jean-Pierre RASKIN , Prof. Sandra SOARES-FRAZÃO

Academic year 2017-2018

Abstract

Worldwide, clean water is increasingly becoming a acutely scarce resource, notably because of toxic organic pollutants such as cytostatic drugs contained in the waterways, which represent a threat to the health and safety of aquatic life. As these pharmaceuticals cannot be removed by conventional wastewater treatments, photocatalytic membrane reactors (PMRs) have recently been proposed as a promising technology to degrade the organic contaminants. In order for this emerging technology to work properly, the membrane module must efficiently retain the photocatalytic particles by operating under suitable flow conditions which minimise membrane fouling and mechanical abrasion caused by the photocatalyst. The investigations on the influence of feed cross-flow velocity (CFV) and feed water composition on the fouling and stability of ceramic membranes in a PMR are presented in this work. Moreover, the filtration efficiency of the fouling cake layer towards small pharmaceutical active compounds (PhACs) is discussed. Alumina (UF-Al_2O_3/ZrO_2) and titania (UF-TiO_2) ultrafiltration membranes with a molecular weight cut-off of 100 kDa, and one titania microfiltration (MF-TiO_2) membrane with maximum pore size of 0,2μm were investigated. Experiments were conducted at constant TMP (3 bar) and fixed TiO_2 photocatalyst loading (1.5 g/dm^3) and by progressively decreasing the applied CFV from 6 to 1 m/s. For all UF membranes, regardless of the membrane compactness and material, increasing the CFV above 3 m/s had no impact on the membrane permeability while working at low CFV (i.e. 1 m/s) led to a significant decrease of the permeability. At low CFV, TiO_2 catalyst concentration in the bulk feed decreased by 65-75% which was attributed to membrane fouling. In case of MF membrane a major influence of the CFV on membrane fouling was observed when the flow was reduced from 6 m/s to 3 m/s. Moreover, the use of wastewater instead of laboratory grade water (LGW) as well as working under more turbulent conditions had almost no impact on the membrane performance in the whole range of CFV (6-1 m/s). Indeed, only the UF-TiO_2 membrane at 3 m/s showed a small reduction of permeate flux with wastewater in comparison with LGW. Additionally, for the UF membranes, the rejection of PhACs was not influenced by fouling cake layer while its selectivity towards small organic compounds was enhanced. After 150h of PMR operation, the UF-Al_2O_3/ZrO_2 membrane did not lose its separation properties at high cross-flow velocity (CFV = 6 m/s).

Acknowledgements

The development of this work throughout this year was analogous to filling the Jar of thesis-life, in which each actor closely or remotely involved added her/his rock, pebble, grain of sand or water droplet to this work. I would like to thank them hereafter in a few words:

The first person I would like to thank is my supervisor, *Patricia Luis* who constituted the bedrock of this thesis-Jar. During the whole semester, she was available to provide her guidance and to answer numerous questions. Additionally, I would like to thank her help in editing and improving the quality of this report.

The second bed of pebbles in this thesis-Jar is *Raphaël Janssens*, without whom this thesis would not have seen light of day. During the whole semester, he dedicated plenty of time to help us in and outside the lab along with his expertise, advice, patience and positive support when facing (so many) unforeseen situations. In addition, his support in writing and editing this paper contributed significantly in the improvement of this report. I would like to personally thank him for all this energy he dedicated to help me achieving the present work.

Then comes the sand in the Jar, which are all the people who provided help and suggestions when a technical issue was encountered with the experimental setup, membrane cleaning in iMAP labs or during the sample analysis in the bio-engineering labs of the ELIM department. *Luc Wautier (iMAP), Hélène Dailly (ELIM labs), Frédéric Van Wonterghem (iMAP), Rony Santoro (iMAP labs) and Nadine Deprez (iMAP labs)*, thanks to all of you for adding your grain of sand to this work by sharing your technical expertise which helped me better understand and solve the problems I was facing.

So far, the thesis-Jar is almost filled but one has to finally add the water to evaluate the permeability of the jar (accomplished work). In that respect, I would like to thank *Pr. Denis Mignon, Pr. Jean-Pierre Raskin and Pr. Sandra Soares* for accepting to be assessors of this master thesis.

Furthermore, I would like to thank my coworker *Maël Makoudi* for all the discussions and the great atmosphere prevailing during our daily lab sessions.

I am also particularly grateful to *Kristina Nangle* and *Pierre Adam* who on a voluntary basis took the time to proof-read my work.

Last but not least there is the shell of the Jar keeping all these previous ingredients together, *family and friends*, which I am very grateful for their moral support all along.

Table of Contents

List of symbols

The next list describes several symbols that will later be referred to within the document's body

Abbreviations

5-FU	5-Fluorouracile
AFM	Atomic Force Microscopy
AOPs	Advanced Oxidation Processes
Cap.	Capecitabine
CP	Cyclophosphamide
ELSD	Evaporative Light Scattering Detector
GAC	Granular Activated Carbon
HWW	Hospital wastewater
IBW	Intercommunale du Brabant wallon
IFO	Ifosfamide
LGW	Laboratory Grade Water
LSM	Laser Scanning Microscopy
MF	Microfiltration
MS	Mass spectrometry
MWW	Municipal wastewater
PC	Photocatalyst
PES	Polyethersulfone
PhACs	Pharmaceutical active compounds
PhCs	Pharmaceuticals
PMRs	Photocatalytic membrane reactors
SEM	Scanning Electron Microscopy

UF	Ultrafiltration
UPLC	Ultra-performance liquid chromatography
WWTP	Wastewater treatment plant

Nomenclature

$\dot{V}_P$	Volume flow	[dm^3/h]
ρ_w	water density	[kg/dm^3]
A_m	Effective membrane area	[m^2]
Abs	Absorbance	[-]
C_f	Concentration of a PhAC/dextran in feed stream	[mg/dm^3]
C_P	Concentration of a PhAC/dextran in permeate	[mg/dm^3]
CFV	feed cross-flow velocity	[m/s]
J_P	permeate flux of the fouled membrane during TiO_2 filtration	[$dm^3/m^2/h$]
J_{LGW}	permeate flux using pure water (LGW)	[$dm^3/m^2/h$]
LOD	Limit of detection	[$-$]
LOQ	Limit of quantification	[$-$]
m_w	mass of permeate (water)	[g]
$MWCO$	Molecular weight cut-off	[Da]
P_m	Membrane permeability	[$dm^3/m^2/h/bar$]
R	Solute rejection coefficient	[%]
R_f	fouling resistance	[m^{-1}]
R_m	membrane intrinsic resistance	[m^{-1}]
R_T	total membrane hydraulic resistance	[m^{-1}]
m/z	mass-to-charge ratio	[-]
pI	Isoelectric point	[-]
TMP	Transmembrane Pressure	[bar]

List of Figures

List of Tables

Introduction

Only 2.53% of water available on earth is freshwater, and it is increasingly becoming an acutely scarce resource in many regions of the world. This is especially true in under-developed countries where 1.2 billion people have no access to safe drinking water and/or sanitation, exposing almost 800 million lives to schistosomiasis[1] [20]. Moreover, are we sure that our european water cycle is safe ? Recent observations and studies conducted over the last decade on hospital wastewater effluents (HWW), municipal wastewater (MWW) as well as surface water showed clearly that even in our developed societies, water treatment should be improved. Studies that analyzed the content of various rivers located near hospitals and urban areas showed a non-negligible and even disturbing contamination of aquatic ecosystems by toxic and xenobiotic substances, the so-called emerging contaminants which include pesticides, industrial compounds, pharmaceuticals (PhCs) and recreational drugs [21].

For the past 20-30 years, the demand and use of PhCs has increased exponentially, especially for the treatment of cancer (antineoplastic/cytotoxic drugs) and other chronic diseases such as type 2 diabetes (metformine, an anti-diabetic drug). In 2017, roughly 14.1 and 46 million new cancer and diabetes cases, respectively, were reported and those figures are expected to double within the next 20 years [22].

Recognising these trends, scientists have been investigating over the last few years an improved sustainable wastewater treatment method for the complete abatement and mineralization of these persistent and increasing quantities of toxic drugs present in the effluents of hospitals. So far, an abatement has been achieved by mean of UV/O_3 advanced photocatalytic oxidation processes (AOPs).

AOPs as part of a PMR system have been operated using TiO_2 as photocatalyst and a UF/MF ceramic membrane showing a high resistance towards mechanical abrasion and interaction with oxidizing species. Although ceramic membranes still lack in rejection efficiency of the cytostatic drugs while their rejecting sustainability is assured.

Several reviews on the subject (*Mozia et al., 2013, 2015*), (*Janssens et al., 2017*), (*Zhang et al., 2016*) have shown that fouling and membrane stability are key points in the development of PMRs. Indeed, up to date, membrane fouling remains the primary setback for the implementation of this technology at industrial scale. Therefore, the objective of the present master thesis is to investigate the rejection performance and stability of alumina ($UF\text{-}Al_2O_3/ZrO_2$) and titania ($UF\text{-}TiO_2$) 100kDa ultrafiltration membranes, and one titania 0,2μm microfiltration ($MF\text{-}TiO_2$) membrane towards TiO_2 particles as a part of an overall PhD project based on PMR technology for the degradation of anti-cancer drugs present in hospital wastewater.

[1] chronic water-borne disease caused by parasitic flatworms which is easily spread by contact with contaminated (fresh)water [20]

This will be achieved by investigating first (RQ1) the hydrodynamics and feed water quality affecting the membrane fouling during PMR operation. Then, (RQ2) the study of rejection efficiency of UF membranes towards anti-cancer drugs will be tackled. Afterwards, (RQ3) focusing on the mechanical abrasion by the photocatalytic particles on UF membrane separation properties over an extended period of time of 150h will be our final step.

Chapter 1

Literature Review

1.1 Hospital wastewater

For the past decade, the pharmaceutical industry has become one of the most prominent economically active industries worldwide amounting to a global market value of US$ 816 billion in 2016 [23]. Among these, the oncology drug market was worth $ 83.2 billion in 2016 and is expected to double to $ 190 billion by 2022 [24]. This can partly be correlated with the increase of cancer cases which counted roughly 14 million new cases in 2012 and is predicted to increase by 70% in the next few decades [21].

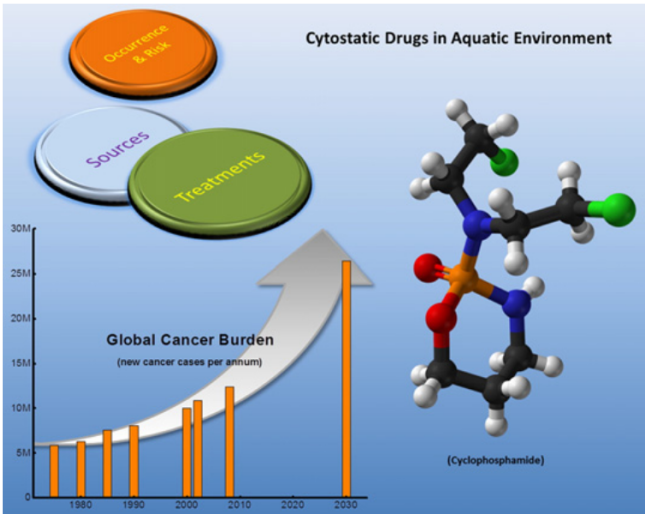

The pharmaceutical industry generates a significant amount of various pollutants. Qualitatively, these pollutants are ranked in three different categories [15]: first there are the domestic discharges (partly originating from personal care products (hygiene, ...) of non-contagious patients and staff). Secondly, the industrial effluents generated by specific equipment (laundry, boiler, air conditioning, workshops, ...) and finally the specific effluents related to healthcare facilities which are produced by the healthcare activities, analysis and research.

The compounds in this last category are predominantly responsible for the presence of pharmaceutical active compounds (PhACs) in hospital effluent(s) . These active substances represent a high environmental risk, and hospital wastewater effluents have been estimated to be between five- and fifteen times more toxic compared to the common municipal wastewater [21]. The different potential routes used by these contaminants to reach the surface or ground waters are illustrated in Fig. 1.1.

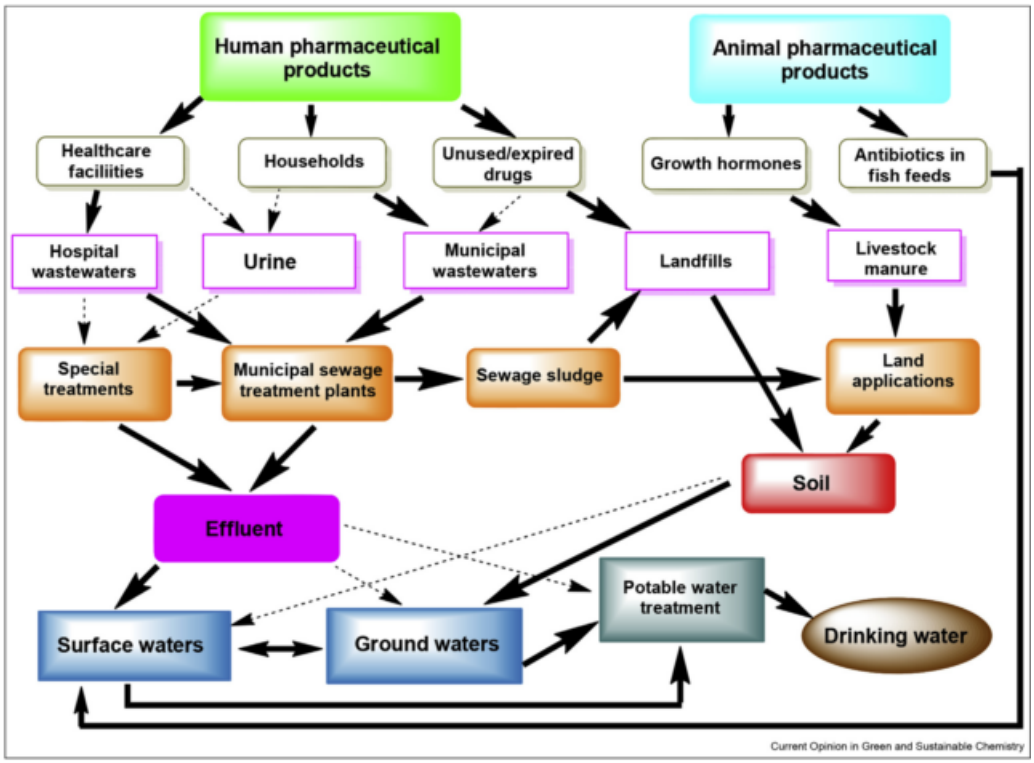

Figure 1.1: Potential routes for human and animal pharmaceutical products to contaminate aquatic environments [1]

1.2 The problem : Pharmaceutical active compounds

The PhACs can be classified in several main categories such as antibiotics, analgesics, anti-epileptics, beta-blockers, X-ray contrast media, steroids and hormones, lipid regulators and cytostatics (chemotherapy drugs) [25]. This last category, namely the cytostatic drugs, are administered to oncological patients to help them treat their cancer and are considered as emerging pollutants. After being partly or completely metabolized by a patient's organism and excreted through urine and faeces, the cytotoxic medication finally reaches the hospital sewage system. The acute toxic effects of these drugs and their intermediates on environmental and human health have already been thoroughly investigated although their chronic effects remain still not well-understood [26]. Therefore, it is critical to deactivate/remove these contaminants from the waterways by means of an appropriate treatment process.

1.3 The remedies : Advanced Oxidation Processes (AOPs)

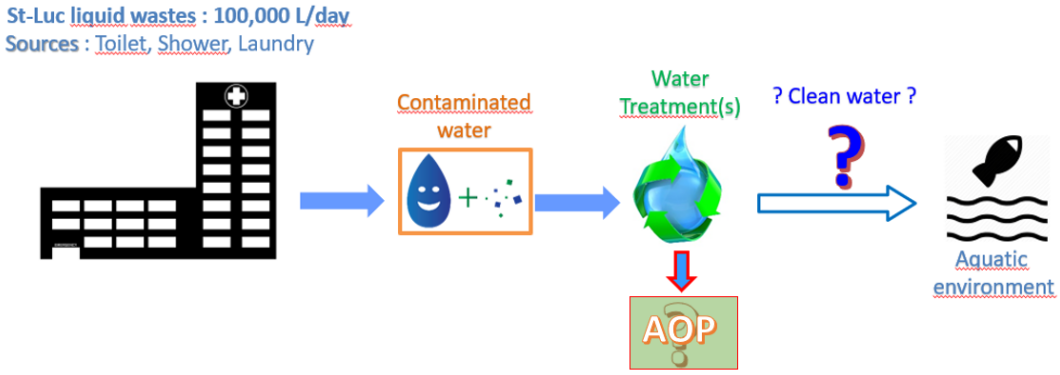

Figure 1.2: Typical hospital wastewater life cycle + AOPs

As showed in the above illustration, the pollutants after being released are treated in a wastewater treatment plant (WWTP). Nowadays, the conventional treatment techniques applied in WWTPs are consecutive primary treatments (coagulation-flocculation-sedimentation), which remove suspended inorganic and some organic particles [27]. Then follows a secondary biological treatment (e.g. moving-bed biofilm process, biofiltration, ANAMMOX process[1], ...) to convert dissolved and colloidal organics into biomass and finally a tertiary treatment (e.g. rapid sand filtration, oxidation, disinfection (UV, O_3, GAC[2] filtration, ...)) is applied for the further removal of suspended solids or nutrients and for final disinfection [28].

These conventional wastewater treatment methods are ineffective at removing these pharmaceuticals as indicated by the trace concentrations of several pharmaceuticals in hospital effluents that have been measured in concentrations ranging from ng/L to low $\mu g/L$ as shown in Table 1.1 and for this reason, AOPs have been developed [21].

Pharmaceutical compound	**dosed concentration (min-max) in hospital effluents** $(\mu g/L)$	
Antibiotics	[MIN]	[MAX]
Ciprofloxacin	<0,038	101
Doxycycline	<0,005	6,7
Penicillin	0,85	5,2
Analgesics		
Diclofenac	0,2	14,9
Ibuprofen	0,069	9
Cytostatics		
Methotrexate	1	1
Cyclophosphamide	0,019	4,5
Ifosfamide	<0,002	1,9

Table 1.1: Bibliographic summary of medicinal pharmaceuticals dosed in HWW effluents [15]

[1] Anaerobic AMMonium OXidation : process for the removal of ammonium from sludge effluents [28]

[2] Granular Activated Carbon is used as adsorption filter for drinking water treatment to remove NOM and micro-pollutants

Chemical treatments for water and wastewater have drawn a lot of attention from the scientific community over the past 30 years and allowed AOPs to see the light of day. Almost 25% of AOPs' research papers (over 4500 articles) published between 2005 and 2007 were devoted to photocatalytic processes according to [29]. Besides being applied to water and wastewater treatment, other R&D journals demonstrated its applicability in other fields as diverse as soil remediation, groundwater treatment, ultrapure water production, volatile organic compound treatment and odour control.

AOPs can be broadly defined as eco-friendly chemical, photochemical or electrochemical phase oxidation methods operating through the intermediacy of highly reactive species ($OH^{\bullet}$ and $O_2^{\bullet -}$ being the most reactive ones) aiming at partly/fully degrading a target pollutant into an innocuous state. Among these mechanisms, we can cite, inter alia, electrolysis, ozonation, Fenton's reagent, ultrasound as well as homogeneous and heterogeneous photocatalysis based on UV or solar visible irradiation [29]. This latter has drawn a lot of attention from the scientific community for its application in water cleaning technology, following physical and biological (pre-)treatments.

Coming back to these drug contaminants (table 1.1), as they cannot be completely removed using conventional wastewater treatments, some authors have proposed to strategically combine conventional treatments with a decentralised solution as the most promising solution for the removal of these organic pollutants [30]. One of them would be to manage human excretions from oncological patients as a separate waste stream with a potential environmental impact [31]. Indeed, as many drugs are predominantly excreted via urine after being metabolized, applying a source-separation strategy for contaminated wastewater streams (e.g. HWW, urine stream) could be an effective way to significantly reduce the discharge of both metabolites and micropollutants into the environment [31]. Moreover, combining urine-source separation strategy followed by smart and cost-effective treatment technology such as a hybrid AOPs + membrane module treatment are strongly investigated nowadays in order to prevent cytostatics from continuously entering surface water [31]. This latter combination is called Photocatalytic Membrane Reactors (PMRs).

1.4 Photocatalytic Membrane Reactors: Photocatalysis && Membrane technology

A PMR is a device existing in various configurations and which combines heterogeneous photocatalysis with a membrane module in order to recycle the photocatalyst in the system.

Depending on the deployed state of the photocatalyst, PMRs can be classified into two main configurations (see Fig.1.3) : (1) Slurry photocatalytic membrane reactors having the catalyst particles suspended in the feed stream and (2) immobilized PMRs having the catalyst immobilized onto the membrane surface. Both reactor types have their distinguishing features and limits.

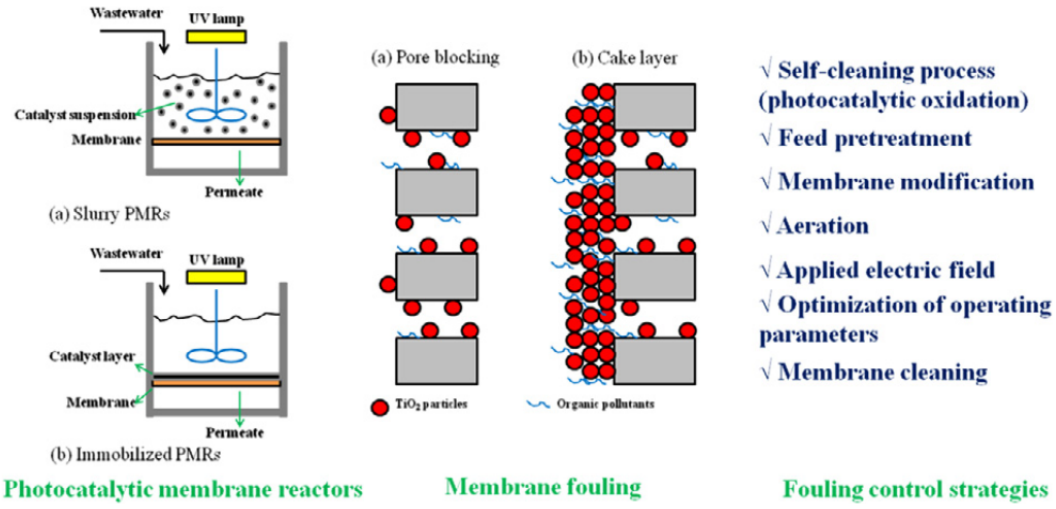

Figure 1.3: PMRs graphical abstract [2]

Immobilized systems are interesting because of the enhanced hydrophilicity of the coated catalyst layer at the membrane surface which would mitigate membrane fouling caused by the different foulants in presence [32]. However, the limited active surface area available for photocatalysis is the main drawback of this configuration and can be solved by using a photocatalyst in suspension ensuring sufficient contact between the catalyst and pollutants to be degraded.

Slurry photocatalytic reactors, by bringing the catalyst in suspension, are very common in wastewater treatment applications but photocatalyst/pollutant fouling remains the major challenge to be overcome. A special attention brought scientific research to find ways to mitigate the impact of this membrane fouling caused by various foulants including catalytic particles, PhACs and their intermediates and also the NOM[3] present in the water.

Slurry PMRs can further be divided in two groups : integratve-type and split-type PMRs. The former combines the heterogeneous photocatalytic process and membrane filtration in one apparatus while the latter

[3]Natural Organic Matter

considers the two processes separately. Dividing the two processes prevents the membrane to be irradiated and hence damaged by UV-light, and this split also facilitates the installation and maintenance of the PMR setup. The present thesis will address the slurry split-type PMR.

The global performance of the PMR is affected by different factors influencing the photocatalysis and the membrane filtration, which are further presented by focusing especially on the membrane module. For more information on the photocatalytic process, the reader will be referred to appendix A.

1.4.1 Heterogeneous Photocatalysis

As tertiary treatment, after physical and biological cleaning measures, heterogeneous photocatalysis is a purification technology which has seen the light of day in 1972 by Fujishima and Honda [5], and which has been extensively studied since and constitutes one of the most promising water treatment technologies [33]. The heterogeneous process consists in a solid-liquid interaction throughout an interface between the photocatalyst and reactants contained within the liquid phase aiming at degrading organic contaminants.

Moreover, this process is termed as a 'Green process' as it helps reducing the use and generation of toxic compounds together with the related risks for the environment and human-health [26]. Several green characteristics of photocatalysis can be outlined such as operating under mild conditions (near room temperature and pressure), abatement of contaminants while mitigating generation of harmful byproducts and use of (chemically) stable photocatalyst(s) (e.g. TiO_2).

A **PHOTOCATALYST** is a semiconductor material able to convert light irradiation energy from a natural or artificial source, into chemical energy of electron-hole pairs inherently part of the material. Hence the ideal photocatalyst must match the following criteria : suitable bandgap energy, chemical and physical stability, available, nontoxic nature and low cost. Many materials match these latter criteria and among these, the most widely used is a nanosized titanium oxide combination as it is the case for *Degussa P25* [16].

Degussa P25 is composed of 20% rutile titania, which is the most stable crystalline structure with respect to anatase and brookite, and 80% anatase titania which has the highest reduction power [34]. In order to activate the photocatalyst, an adequate radiation source within the exciting range of the photocatalytic material is required. For TiO_2, the bandgaps of anatase and rutile are provided in table 1.2. Nowadays, a lot of research is made to shift the absorption spectrum of PCs towards visible light ($400 < \lambda < 700$ nm) by doping with anions (N, F, C and S) or noble metals (Au, Pd, Rh, Ni, Cu and Ag) as the absorption spectrum of titania is too low (λ_{abs}<400nm).

Semiconductor	**Bandgap** (eV)	**Bandgap wavelength** (nm)
TiO_2 anatase	3.2	387
TiO_2 rutile	3.0	380

Table 1.2: Bandgaps energy and wavelengths of polymorphous TiO_2 [16]

The photocatalytic mechanism responsible for the photodegradation of pharmaceutical compounds by excitation of a photocatalyst (e.g. TiO_2) can be roughly described as follows:

$$\text{Organic molecules (PhCs)} \xrightarrow[\textit{partial degradation}]{OH^{\bullet}} \text{Oxidation products} \xrightarrow[\textit{Mineralization}]{OH^{\bullet}} \text{Harmless species (e.g. minerals)}$$ [4]

In order for this heterogeneous photocatalytic process to work in a continuous and more effective way, it can be combined with membrane technology so as to recover and reuse the catalyst particles in the process. The design of this hybrid system depends both on the type of photocatalyst which has already been discussed but also on the membrane module, which is now apprehended.

1.4.2 Membrane filtration module

Membrane processes could be broadly defined as modern physico-chemical separation techniques using differences in permeability (of water constituents) as a separation mechanism. Typically, the membrane is said to be semipermeable because it is highly permeable to some compounds present in the feed and less or not permeable to others, which form the retentate stream as illustrated in Fig. 1.4. As result, the permeate stream is relatively free of impermeable constituents whereas the retentate stream is concentrated in those compounds. In membrane filtration, water forces its way through a thin porous layer of polymer or ceramic material. So, the filter itself consists in a continuous mass with tortuous interconnecting voids of different sizes as can also be seen in Fig. 1.5. The common configuration in water treatment for ceramic membranes is a tubular "in-out" single- or multi-channel membrane configuration operating in cross-flow filtration. This configuration influences the packing density[5] and hence the cost profitability which will be approached in 1.4.2.

[4] Mineralization aims at converting C to CO_2, H to H_2O, N to Nitrate, S to Sulphate, P to Phosphate and Cl to Chloride

[5] the membrane area per unit volume in a membrane module [35]

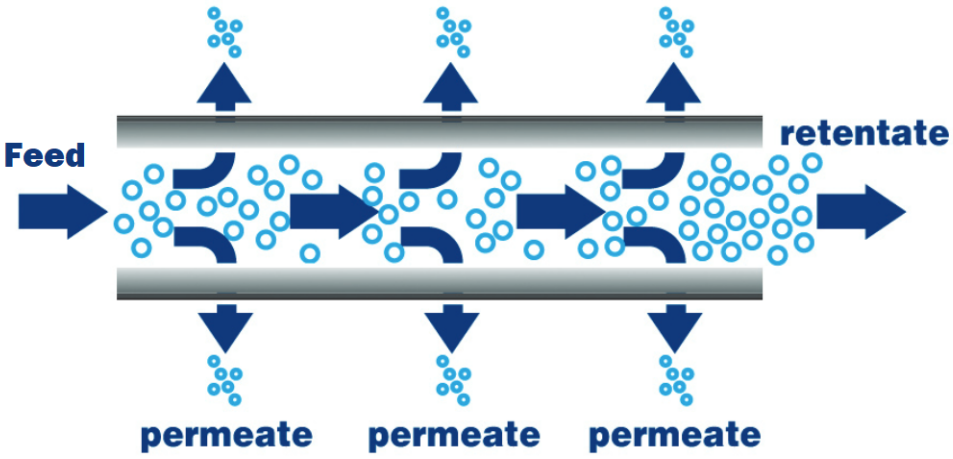

Figure 1.4: Membrane filtration in tubular membranes [3]

The application of an adequate membrane is vital to the synergy of PMR performance. Several parameters must be considered for the membrane process including membrane porosity, membrane material and also the membrane configuration, which are now presented.

Membrane material

The membrane material must be meticulously chosen since the UV irradiation, reactive oxygen species and the photocatalytic particles could damage the membrane module. Among these, the mechanical abrasion of membrane surface by photocatalyst was found to cause more damage to the membrane separation properties than the action of oxidizing species [33]. On the market, two main types of membrane materials can be found : organic (i.e. polymer) and inorganic (i.e. ceramic) membranes. On the one hand, polymeric membranes are the most intensively used up to date as they are relatively affordable but have a short lifespan as they are not so robust against mechanical abrasion by photocatalyst and chemical cleaning agents, which makes the membrane cleaning more difficult. Indeed, the repetitive contacts by catalyst particles with the surface weaken polymeric membranes by abrasion. Furthermore, these organic membranes are more prone to fouling. On the other hand, ceramic membranes consist of rigid monolithic elements which are hydrophilic[6], rough, and are able to withstand high temperature and pressure. They also present a good stability towards chemicals ,pH change and ultrasonic irradiation, and therefore, can be cleaned using more aggressive cleaning techniques (e.g. strong acid/base, sonication, ...) [37]. The different cleaning methods will be more deeply approached in subsection 1.4.5. However, the high manufacturing cost of ceramic membrane curtails their application at industrial scale. Indeed, ceramics are 10-20 times more expensive (per unit membrane area) compared to polymeric ones. In the case of PMRs, ceramic membrane shows a better resistance against photocatalytic reactions and scouring action of the photocatalytic particles, making it the material of choice for PMR operation [36].

[6]Hydrophilicity indicates how a water drop spread across a material surface [36]

To sum up, we have on the one hand a **ceramic** robust, fouling-tolerant, easy to clean but expensive membrane while on the other hand we have a **polymeric** affordable but less robust and fouling resistant membrane.

Membrane filtration in UF/MF

Different groups of membranes can be distinguished based on the driving forces involved. On the one hand, we have concentration and partial pressure separation processes such as dialysis, pervaporation and membrane distillation. On the other hand, pressure-driven processes including reverse osmosis, nanofiltration, ultrafiltration (UF) and microfiltration (MF) membrane techniques where a solvent and a various range of solutes will pass through the membrane or be (partly) rejected depending on the membrane structure. The hierarchy of this latter category and their respective characteristics are shown in Fig. 1.6. This classification is based on the types of materials rejected, operating pressures, molecular weight cut-off (MWCO) and nominal pore dimensions [38].

Most of the time, for PMR operation, UF and MF filtration membranes are asymmetrically structured as they consist of several layers [9]: active dense top layer of fine particles , an intermediate layer(s) of larger particles and a thick porous support as illustrated in Fig. 1.5. As UF membranes have a dense surface layer, it is difficult to characterize them by means of a true pore size distribution. For this reason, one characterises them by their MWCO. The MWCO of a solute being the minimum molecular weight of this latter in order to obtain a 90% rejection in a membrane separation process. Typically UF membranes are designed to retain molecular sizes in the range of 1 kDa - 1000 kDa which is roughly corresponding to an "equivalent" pore diameter range of 1 - 100 nm [38].

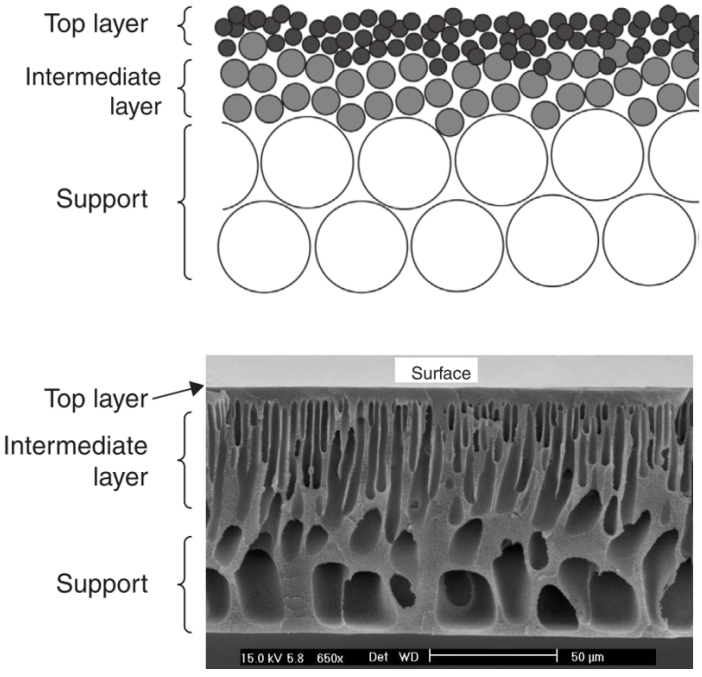

Figure 1.5: Scheme of a TiO_2 ceramic asymmetric membrane. Figure modified from [4]

According to their use in water treatment, two distinct physico-chemical classes of membrane processes exist : membrane filtration (porous) and reverse osmosis (non-porous[7]). In PMRs the primary function of the membrane is to retain «large» catalytic particles in the range of 5-100 nm for which UF and MF membrane can achieve high separation efficiency and therefore, narrower pore range (NF and RO) is not required [33]. Further through this review, membrane filtration which encompasses MF and UF will be presented.

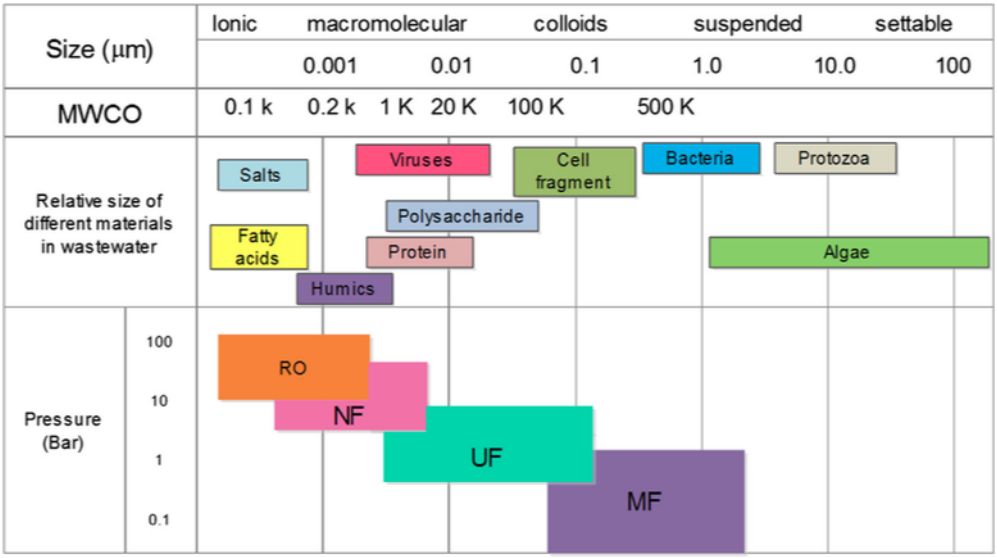

Figure 1.6: Various pressure-driven membrane processes [5]

Focusing now more specifically on membrane filtration, which can be defined as a process separating suspended particles from a liquid phase by retention of those particles by a porous media (such as a membrane). The filtration mechanism for MF and UF consists in size-exclusion (i.e. straining/sieving mechanism). Consequently, membrane filtration aims at separating a dispersed solid phase (e.g. catalyst) from the two-phase feed stream system which is larger than the size of the pores in order to produce a water stream «clean of any suspended solid».

Operating modes

The membrane filtration can be operated in two distinct modes shown in figure 1.7. The dead-end mode uses high packing density membranes which promotes filter cake formation on the membrane surface able to clog the membrane and by doing so, reducing the filtration performance. For the cross-flow (tangential) mode, the feed on the upstream side of the membrane is transported parallel to the membrane surface and the permeate on the downstream side flows away in the direction normal with respect to the membrane surface. The main advantage of cross-flow filtration over dead-end being the removal of fouling along with the retentate stream recycling to the feed and is therefore preferentially used in PMRs in order to minimise

[7]NF and RO are considered as non-porous membrane processes since their separation mechanism is not based on size exclusion but on differences in solubility and diffusivity

membrane fouling.

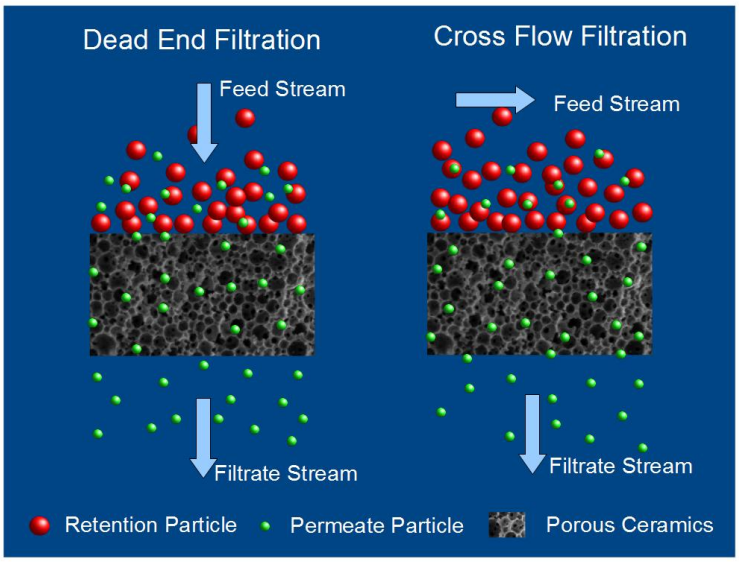

Figure 1.7: Membrane operating modes [6]

1.4.3 Filtration mechanisms

As a reminder, the primary role of a membrane module is to filter and reject components and in our case, the photocatalytic particles and ideally also the contaminant along with its degradation by-products. Hence, a review of the different membrane filtration mechanisms seems useful. Not to mention that after some time fouling arises through these three main mechanisms which govern membrane filtration [35]:

1. **Straining** (sieving) is the dominant mechanism occurring when particles of size larger than pore size of the membrane are physically retained on the membrane surface
2. **Adsorption** happens within the pores by adsorption of small organic material on the pore walls and can thereby block the further passage of other particles.
3. **Cake filtration** consists in the retention/accumulation of small particles by a cake composed of larger material. Hence in the case of a dense cake layer formed due to organic deposition, this cake acts as an additional filter medium.

In membrane filtration, the retained species tend to accumulate over time at the membrane surface, hence limiting the permeate flux which is counter-balanced by back-diffusion.These phenomena are known as concentration polarization and fouling. The study of this permeability reduction and its root causes **in PMRs** are still not well understood by the scientific community which is why this topic is worth being further investigated through this work. Before looking at the operating parameters which might influence

the severity of the membrane fouling, a short review on the fouling mechanisms will be introduced in the next section as well as the several remedies, the so-called cleaning mechanisms, performed up to date.

1.4.4 Membrane fouling

It is known that the main technical barrier still to be overcome in order to commercialise PMRs for large scale applications is membrane fouling.

Membrane fouling corresponds to the adsorption and/or deposition of foulants on/in a membrane surface/-pores and consequently leading to a decline in membrane permeability [5].

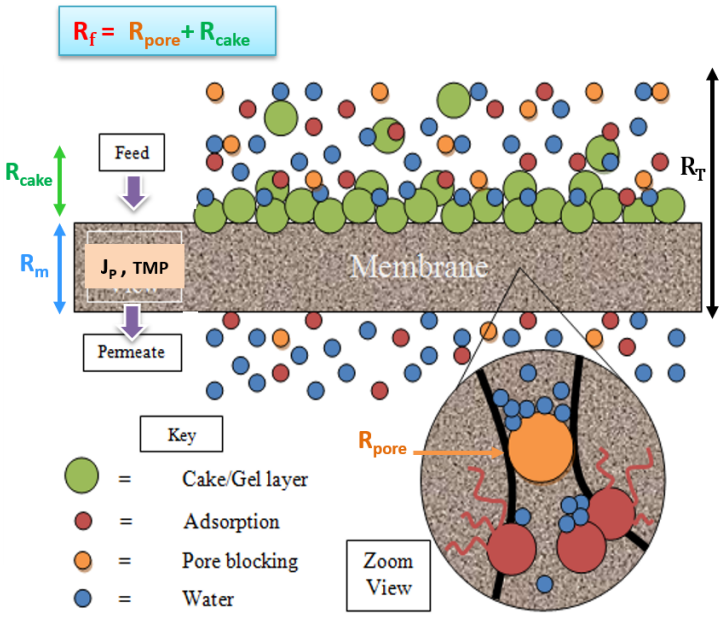

Figure 1.8: Membrane fouling mechanisms in PMR operation. Figure modified from [7].

During PMR operation two main foulants have to be accounted for : organic pollutants (e.g. PhACs, dextran) and photocatalyst particles (i.e. TiO_2) which in turn may interact with the membrane surface, and thereby influence significantly the fouling formation during membrane filtration. Besides, there is no report of occurring in PMRs of bio-fouling or scaling, which are two other foulants encountered in membrane processes.

Organic and inorganic foulants can foul the membrane in two different ways as illustrated in figure 1.8: (1) reversibly (porous layer) or (2) irreversibly (pore blocking and/or dense cake layer) [8].

The first one relates either to the agglomeration of the photocatalyst nanoparticles (up to microscale) which in absence of organic pollutants forms a thick porous cake layer on the membrane surface as illustrated in Fig. 1.9 (left). This cake layer has a low resistance for water flux causing no significant flux decline and which

[8] Also called removable and irremovable fouling, depending on the authors

can be cleaned by a physical backwashing technique [9]. Or in absence of photocatlayst particles, a dense but reversible organic (gel) layer by means of concentration polarisation could develop at the membrane surface driven by the difference of concentration of soluble organic pollutant between the membrane surface and the bulk feed [37].

The second fouling mechanism takes place in two subsequent stages :

- First membrane **pore blocking** can occur by either the adsorption/deposition of organic pollutants on the pore walls and/or by the accumulation of small catalyst particles on/into the pores as shown in Fig. 1.8. As most organic compounds are hydrophobic in nature (e.g. dextran, PhACs), they attach more easily on/inside the hydrophilic membrane surface/pores and therefore causing more severe fouling. This internal fouling can only be removed by chemical cleaning.
- Then, a **dense cake layer** can form on the membrane surface due to the adsorption of a small amount of organic pollutants onto the TiO_2 photocatalytic particles as shown in Fig. 1.9 (right). These organic pollutants penetrate into the voids left in between the large TiO_2 particles and therefore increasing the cake density which in turn causes a flux decline.

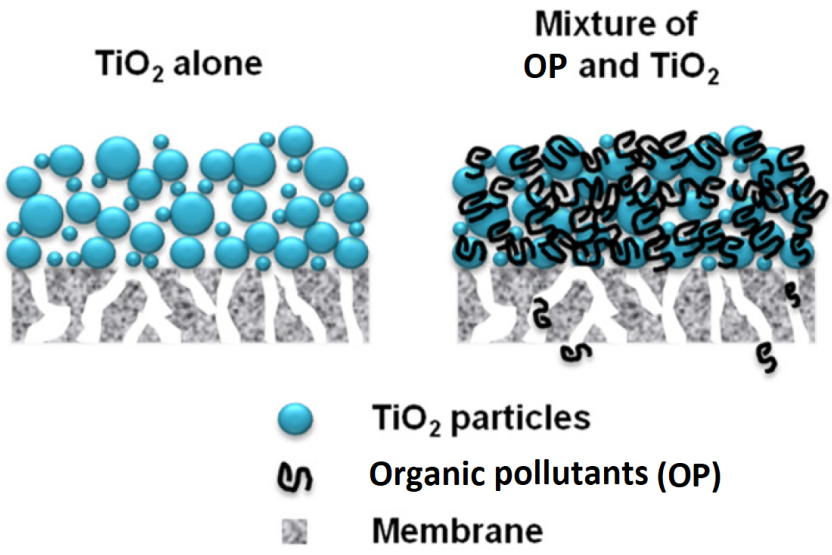

Figure 1.9: Membrane fouling caused by TiO_2 particles alone and mixture of organic pollutants and TiO_2 particles. Figure modified from [8].

As a consequence of this complete/partial pore blocking and cake layer build-up on the membrane surface by the interaction between organic and inorganic foulants, the size of the pores are narrowed and/or completely blocked. Therefore, the performance of PMRs are seriously hindered. However, the development of a dense cake layer on the membrane surface enhances the retention of smaller compounds in the process.

Especially in the case of PMR, the use of UV-light during operation has shown to have a significant impact on membrane fouling. Indeed, without UV-light, no photocatalysis is occurring and hence organic matter

by means of concentration polarisation forms a dense layer at the membrane surface. In contrast, when switching ON the UV lamps, organic pollutants are decomposed and organic fouling is alleviated, hence decreasing pore blocking.

Influencing factors on PMR performance

The rate at which fouling occurs during PMR operation is affected by several parameters including the pore size and its distribution, the nature and concentration of foulants (e.g. PhACs, NOM, ...), the membrane materials and surface characteristics (i.e. pH), and finally the hydrodynamics play a major role in the control of fouling. So far, several of these impacting factors have already been approached in section 1.4.1 dealing with photocatalysis in order to evaluate their effect on the degradation mechanism. Hereafter, the factors influencing the permeate quality in PMR using TiO_2 as photocatalyst are summarised :

1. The Transmembrane Pressure (TMP) : at high TMP, presence of TiO_2 nanoparticles increases significally the fouling causing a decrease of the permeate flux.
2. The feed Cross Flow Velocity (CFV) : high cross flow velocity leads to high shear rates, which hinder the build-up of the polarisation layer
3. The concentration of NOM in the feed solution : a severe membrane fouling is being caused by strong interactions between catalyst and organic particles. This flux can however be restored in presence of UV light due the decomposition of these organic particles
4. The pH value of the feed solution : if pH<pI[9], the adsorption of negative charges pollutants like organic pollutants is facilitated, but if pH>pI, then positive charged particles tend to adsorb on the TiO_2 particles. The fouling is minimised at pH around 6,8 (i.e. pI of TiO_2)
5. Superhydrophilic effect: during UV irradiation, TiO_2 catalyst particles gain superhydrophilic properties which further leads to an improvement of the water permeability
6. The photocatalyst concentration [TiO_2] : higher catalyst concentrations lead to greater permeate flux decline
7. Size of the photocatalyst particles : larger TiO_2 particles exhibit less fouling tendency

[9]The isoelectric point (pI) characterises the neutral ionisation state of the catalyst surface which determines adsorption efficiency of organic pollutant.

1.4.5 Fouling control strategies

Now that the PMR related fouling mechanisms have been presented, different strategies to tackle the fouling problem in order to inhibit the fouling formation can be adopted. A great arsenal of strategies exist such as membrane doping, aeration (bubbling) and hydrodynamics optimisation, which are further discussed in appendix B. The most common one at lab and industrial scale, i.e. membrane cleaning, is hereinafter discussed and will be further approached in the chapter dealing with the cleaning procedures in Chapter 3 (3.3.2).

A great variety of membrane cleaning methods are used nowadays such as sonication, ozonation, electrification, and enzymes which are non-conventional methods but up-to-date two conventional procedures can be distinguished from the others: physical and chemical cleaning. Usually physical cleaning is applied in case of reversible fouling whereas the use of chemicals comes into play in case of irreversible fouling. Moreover, a combination of the two is often applied so as to more effectively clean the membrane.

Physical cleaning consists in a (gas) backflushing procedure. This backwashing process consists in a reversed flush membrane backward from the permeate side to the feed side, hence expelling TiO_2 particles as well as organic foulants by inversing the TMP. Additionally, the backflush also loosen fouling cakes stuck on the membrane surface.

On the other hand, with **chemical cleaning**, the choice of (the right) chemical for cleaning depends on the nature/type of foulant [37]. If this latter is an organic foulant, an alkiline solution will be used while an acid solution is relatively effective to remove inorganic foulants. In most cases, a multiple step strategy has to be applied in order to recover the membrane's permeability because of the organic/inorganic cocktail of foulants.

Membrane cleaning is far from being a simple process by applying a sole universal cleaning method. Different methods and chemicals can be used depending on the feed product, the membrane and the interaction between both. The operating conditions have also an impact as explained in the previous section (1.4.4).
The main setback towards the implementation of these strategies remains their high operating cost and the membrane unavailability during the cleaning process.

1.5 State of the art on membrane fouling during PMR operation

There has been a growing interest in PMRs for water treatment in the past few years accounting for 90 publications on that subject in 2016 [33] and lots of them specifically deal with membrane fouling. *Mozia et al.* [9] already studied a slurry PMR system using TiO_2 P25 photocatalyst and TiO_2 FILTANIUM ceramic MF and UF membranes with respective pore size of 0.2μm and 100 kDa. They focused their study on the effect of several operating parameters, i.e. feed cross-flow velocity, transmembrane pressure and catalyst loading, on the stability and fouling of the membranes in a PMR. During their study, they found out that the CFV and the concentration of TiO_2 in the feed had no effect on the permeability of the membrane ranging respectively from 3 to 6 m/s and 0.5 to 1.5 g/L. By contrast, the MF membrane experienced a permeability decline with decreasing the CFV which the authors attributed to membrane pore blockage by the catalyst particles.

During their study, *Mozia et al.* observed that the permeability of all UF membranes increased compared to pure water flux **during PMR operation** regardless of the hydrodynamic conditions. However, after performing long-run rejection tests with dextran (70 kDa (UF), 2000 kDa (MF)) to verify the separation characteristics of the membrane **after PMR operation**, no decline in the filtration efficiency of the UF Filtanium 100kDa membrane was observed (Fig.1.11a). Hence the authors concluded that for this unique UF membrane the catalytic particles were able to deposit into the pores, hence causing no damage to the separation surface layer.

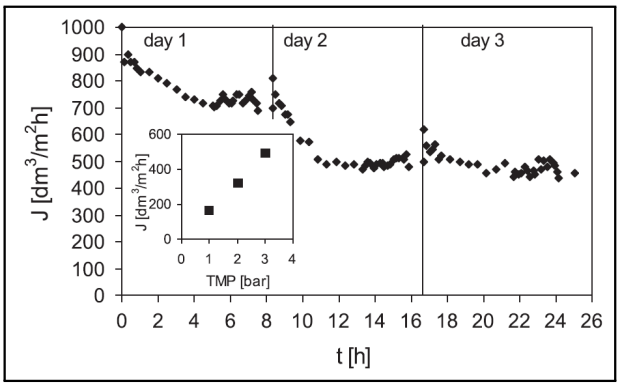

(a) Change of permeate flux for 100kDa Filtanium UF membrane

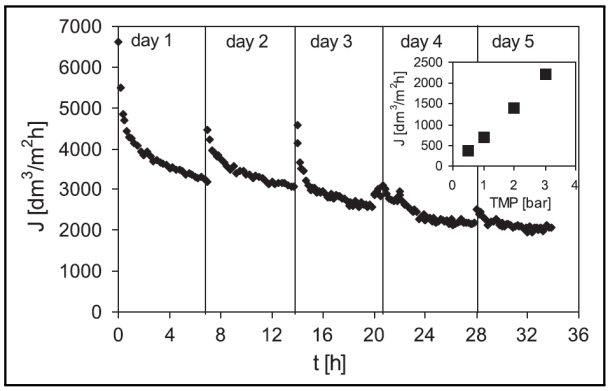

(b) Change of permeate flux Filtanium 0.2μm MF membrane

Figure 1.10: Change of permeate flux during (a) **UF (100kDa)** and (b) **MF (0.2μm)** of pure water at TMP of 3 bar [9]

For the MF membrane, the rejection doubled after 50h of operation due to the agglomeration of the photocatalyst particles and their deposition on/inside the membrane surface, hence forming an additional porous filtration layer. Indeed, the brand new membranes initially tested by *Mozia et al.* [9] with pure water experienced a permeability decline with time, as can be seen on Fig 1.10, ranging from 900 to 500 dm^3/m^2/h for UF membrane and from 5500 to 2000 dm^3/m^2/h for the MF one. They related this decline to membrane wetting. Indeed, the authors evidenced that membranes kept dry showed higher permeate flux regarding hydrated ones, hence causing a permeability decrease over time until getting stabilised. Therefore, to avoid an initial permeability decline, membranes should be immersed in water before starting the experiments.

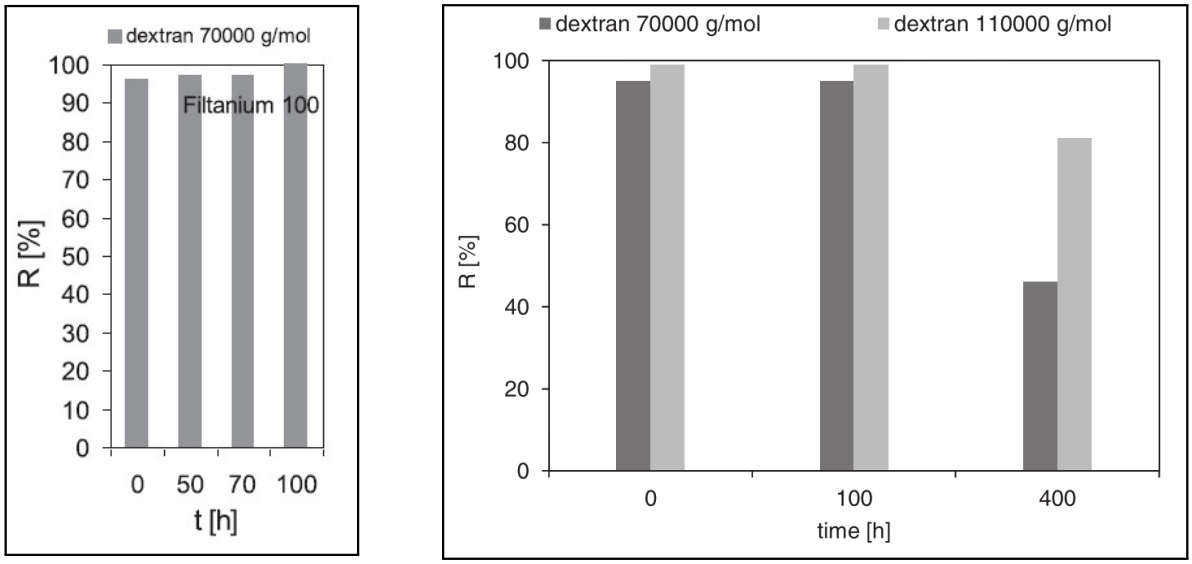

(a) Changes of separation properties after 100h operation in PMR

(b) Changes of separation properties after 400h operation in PMR

Figure 1.11: Changes of separation properties of Filtanium 100kDa membrane after (a) 100h and (b) 400h operation in PMR reprinted from [9] and [10] respectively

According to [9], [32] and [8], this cake layer formed on top of the membrane skin layer at low flow velocity presented a dense structure which could further improve the rejection of smaller particles by acting as a "secondary dynamic membrane". The presence of this cake layer was confirmed by *Mozia et al.* by analyzing the UF membrane surface using SEM as shown on Fig. 1.12

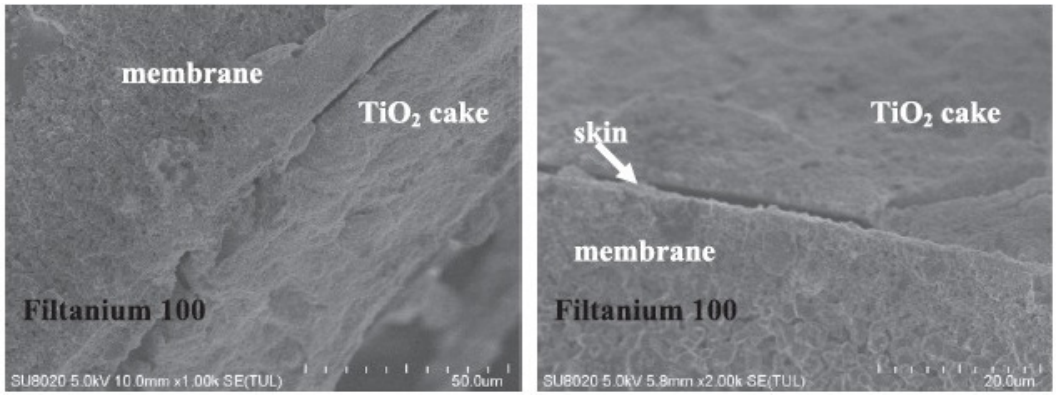

Figure 1.12: SEM microphotographs of Filtanium 100kDa cross-section after experiments in PMR conditions by *Mozia et al.* [9]

The long-run filtration test was also performed by *Szymański et al.* [10] on the Filtranium 100 kD membrane during 400h this time and using the same probe sugar as [9]. The results obtained showed a decrease of rejection from 95 to 46% for 70 kDa and 99 to 81% for 110 kDa dextrans. In both cases, they observed no change in separation properties after 100h (Fig.1.11b) of continuous operation, and even after more then 2 weeks, the membrane skin layer had not been entirely stripped off by scouring of the photocatalyst (no significant change in the layer's thickness) despite the high/small rejection decrease as can be seen on Fig.1.13. The first observation emphasises the fact that the mechanical abrasion of the membrane separation layer by TiO_2 particles is a slow process. Furthermore, since the skin layer was not completely damaged, this decrease of rejection could be predominantly attributed to the opening of new pores by the catalytic particles.

The procedure to calculate the rejection will be further introduced in subsection 3.4.2.

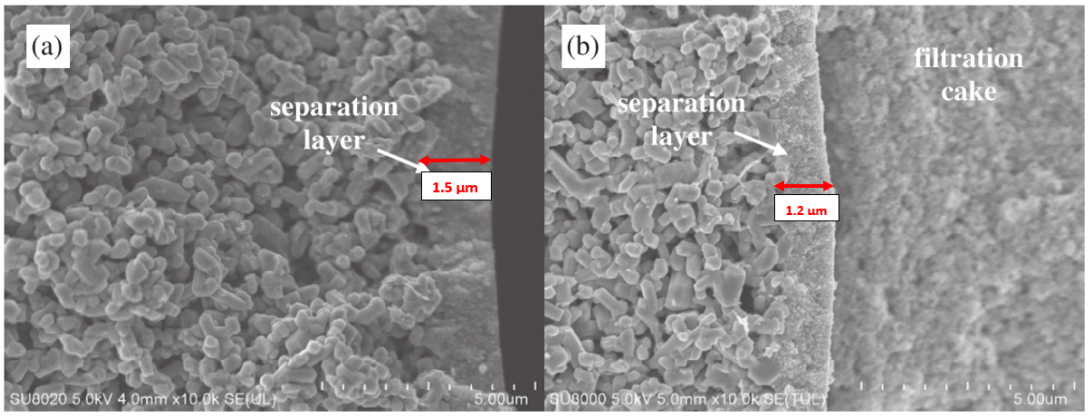

Figure 1.13: SEM cross sections of 100 kDa UF membrane before (a) and after (b) 400h of operation in PMR [10]

Regarding specifically the filtration of pharmaceuticals, *Ganiyu et al.* [39] studied the different mechanisms of rejection of pharmaceuticals in membrane filtration. Since for MF/UF size exclusion is the prevailing retention mechanism, the authors concluded, that MF/UF processes could only be used as pretreatment processes as most PhACS are much smaller (<400 Da [40]) than the MWCO of most MF/UF membranes . Moreover, in PMR operation these pharmaceuticals are degraded by photocatalysis resulting in even smaller by-products resulting from their decomposition [41]. However, when moving to smaller pore sizes for UF (close to NF range), additional separation mechanisms would come into play (i.e. hydrophobic/adsorptive mechanism and electrostatic interaction) and hence improve the membrane selectivity [42].

Filtration resistance model

The cake layer formed during PMR operation on the MF/UF membrane surface creates an additional resistance for water permeation. This filtration resistance can be modelised using the resistance-in-series model which is a very common and simple model used to quantify the contribution of each fouling mechanism to overall flux decline ([43], [8], [44], [42],[45]). The filtration resistance is analogous to the reverse of the membrane permeability and the different resistances contributing to the permeability decline are shown in Fig.1.8. It is worth noting that in this model, the two main fouling mechanisms considered in PMR, i.e. cake formation (R_{cake}) and pore blocking (R_{pore}), are combined into one unique fouling resistance R_f [8].

The general corresponding equations to evaluate fouling are :

$$J_P = \frac{TMP}{\mu \cdot R_T} \quad [dm^3/m^2/h] \tag{1.1}$$

$$\begin{aligned} R_T &= R_m + R_{cake} + R_{pore} \quad [m^{-1}] \\ &= R_m + R_f \end{aligned} \tag{1.2}$$

where J_P is the permeate flux at the end of the filtration experiment in [dm^3/m^2/h], μ the viscosity of the feed solution in [$bar \cdot s$], TMP the transmembrane pressure [bar] and R_T the total hydraulic resistance which consists of the intrinsic membrane resistance R_m and the fouling related resistance R_f in [m^{-1}], the former being calculated using the following equation :

$$R_m = \frac{TMP}{\mu \cdot J_{LGW}} \quad [m^{-1}] \tag{1.3}$$

with J_{LGW} the permeate flux in LGW[10] conditions in [dm^3/m^2/h].

[10]Laboratory Grade Water (presented in chapter 3)

Further in this work, the membrane permeability will be used to characterise the membrane separation properties, hence equations 1.2 and 1.3 can be expressed in terms of membrane permeability (P_m) which is defined by Darcy's law in equation 1.4 :

$$P_m = \frac{J_P}{TMP} \qquad [dm^3/m^2/h/bar] \tag{1.4}$$

$$R_T = \frac{1}{\mu \cdot P_m} \qquad [m^{-1}] \tag{1.5}$$

$$R_m = \frac{1}{\mu \cdot P_{m-LGW}} \qquad [m^{-1}] \tag{1.6}$$

with P_{m-LGW} the membrane permeability of LGW in [dm^3/m^2/h/bar].

In their study [45], *Zuriaga et al.* calculated their resistances using permeate flux and TMP = 3 bar and the viscosity of the solution was assumed to be the same as the water at 20°C operating temperature :
$\mu_w = 1.05 \cdot 10^{-8}$ [$bar \cdot s$].
The intrinsic membrane resistance (R_m) using equation 1.6 was carried out by filtration of demineralized water and then the total resistance (R_T) was obtained using equation 1.5 by operating in PMR conditions hence promoting the fouling conditions.

It should be mentioned that generally, for PMR operation, three resistances have to be accounted for including the cake resistance R_{cake}. This resistance is determined in other papers by experimentally performing a pure water filtration after removing the cake layer formed during the R_T step. However, in this study, to further simplify this model, we have assumed this cake resistance as being part of the fouling resistance R_f and calculated this latter by finally subtracting the two others: $R_f = R_T - R_m$ [45].

Chapter 2

Objectives

At this point, concerns about PhACs as water pollutants and the scientific background in order to deal with this environmental threat have been acquainted with. The broader frame of which this master thesis is part of will be addressed as well as the objectives and research questions this thesis will try to answer to.

This paper focuses on one part of the PhD thesis of *Raphaël Janssens* supervised by Prof. *Patricia Luis* entitled: « *Hospital wastewater treatment : Removal of anti-cancer drugs from WW by AOPs* ». The membrane module as a part of the slurry PMR setup under study in the doctoral thesis will be the core of this work.

The general objective of this master thesis is to study the rejection performance and stability of ceramic ultrafiltration/microfiltration membranes towards TiO_2 photocatalytic particles in a PMR. This study will be performed using TiO_2 and Al_2O_3/ZrO_2 membranes which are further presented in this work. In order to fulfil this objective, **research questions** have been established for which one yearn to find answers throughout this study:

1. How is the membrane fouling affected as per the hydrodynamics and water matrices using MF/UF ceramic membranes in a photocatalytic membrane reactor?
2. Which contribution provides the membrane cake layer formation to the separation properties towards PhACs and dextran using TiO_2 MF/UF membranes in a PMR ?
3. How is the stability of the separation properties using Al_2O_3/ZrO_2 ceramic membrane during PMR operation affected over long-term operation ?

and finally, future research perspectives will be given with the aim of further improving the scientific knowledge in this field.

Chapter 3

Materials and Methods

The experimental methodology, the setup, the related equipment as well as the chemicals which have been used to perform the experiments are presented below. This chapter also includes the background and methods used to analyse the samples. The methods are in line with those used by other authors in this field, among them *Mozia et al.* [9].

3.1 Materials

3.1.1 Water matrices

For the pure water flux tests, all the feed solutions were prepared using demineralized water devoid of heavy metals and inorganic ions. This type of water corresponds to type II laboratory grade water (LGW) and will be further referred to in this work as **LGW**.

In the second part of these experiments, treated wastewater from the WWTP of Court-St-Etienne (IBW[1]) was used to evaluate the impact of the water matrix on membrane fouling. The composition of this wastewater is presented below along with the discharge standards specific to the plant. As one can see, the values for phosphorus and orthophosphate are quite above the standards which could be explained by the fact that the water sample only underwent primary (suspended solids-removal) and secondary treatments (nitrogen-removal, BOD-removal) [17]. Indeed, in this case, all evidence points towards the lack of chemical dephosphatation as a final step for wastewater treatment.

[1] Intercommunale du Brabant wallon

Discharge standards for biological water treatment (WWTP Court-St-Etienne) (Dry weather)		WW composition (OUT) (WWTP - Court-St-Etienne) 21st March 2018	
BOD5	5 mg/l	BOD5	0,5 mg/l
COD	125 mg/l	COD	10,7 mg/l
SS	35 mg/l	SS	0 mg/l
N_{tot}	10 mg/l	N_{tot}	5,42 mg/l
NH4	5 mg N/l	NH4	0,23 mg N/l
P_{tot}	1 mg/l	P_{tot}	3,2 mg/l
Orthophosphate	0,5 mg P/l	Orthophosphate	3.15 mg P/l

Table 3.1: Composition of wastewater at outlet of the WWTP of Court-St-Etienne according to IBW [17]

3.1.2 Catalyst

Degussa Aeroxide® P25 (EVONIK) was used as a photocatalyst composed of 80/20wt.% anatase/rutile TiO_2. This catalyst had similar physico-chemical properties as the titanium oxide ceramic membranes (*Filtanium*) studied. The average particle size of the catalyst is 21 nm.

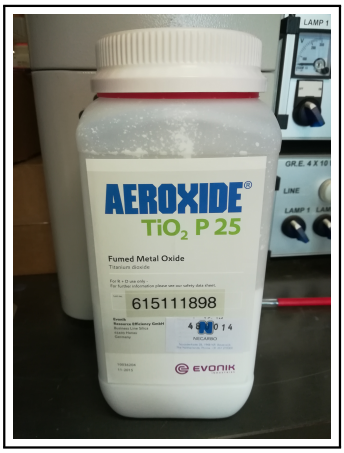

Figure 3.1: TiO_2 Degussa Aeroxide photocatalyst

3.1.3 Filters

Polyethersulfone (PES) syringe filters VWR® with pore size of 0,2 μm have been used to filter the fine catalytic particles contained in the feed samples taken during the experiments involving the four PhACs under study. Indeed, the raw sample from the feed contains water, PhACs and TiO_2 particles. It is mandatory to remove the photocatalyst prior the analyses of the pharmaceuticals by UPLC/MS.

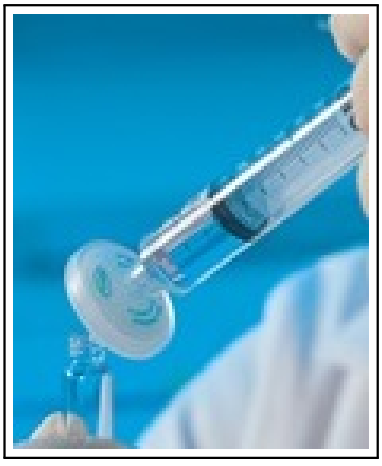

Figure 3.2: VWR® PES syringe filters

3.1.4 Membrane modules

The experiments were performed on six tubular ceramic membranes (see Figure 3.3) that are presented below along with their attributed code name by which they will be further referred to in this work:

- **TiO_2** FILTANIUM™(TAMI Industries)
  - **UF-TiO_2-1Ch**: 1 channel UF membrane with MWCO = 100 kDa
  - **UF-TiO_2-7Chs**: 7 channels UF membrane with MWCO = 100 kDa
  - **MicroCh**: MF membrane with a maximum pore size = 0.2μm
- **Al_2O_3/ZrO_2** ATECH : **Al95 and Al72**: two UF membranes with MWCO = 100kDa

Figure 3.3: Pictures of the *Filtanium* and *Atech* membranes under study

The dimensions of the 1 channel membranes were 25cm in length with an external/internal hydraulic diameter of 10mm/6mm. The effective membrane area (A_m) was 0.0047 m^2. For the 7 channels membrane, the internal hydraulic diameter of each channel was 2mm, providing an effective membrane area of 0.0132 m^2. In this setup, the membrane was placed in a 25cm long metal housing structure with a diameter of 15 mm (ATECH). The housing structure constituted a Tetris T-shape with the long hollow part in which the membrane was placed and the small protrusion through which the permeate flowed out to then be recycled into the feed tank via a plastic hose placed in between (see Fig. 3.4).

3.2 Experimental setup

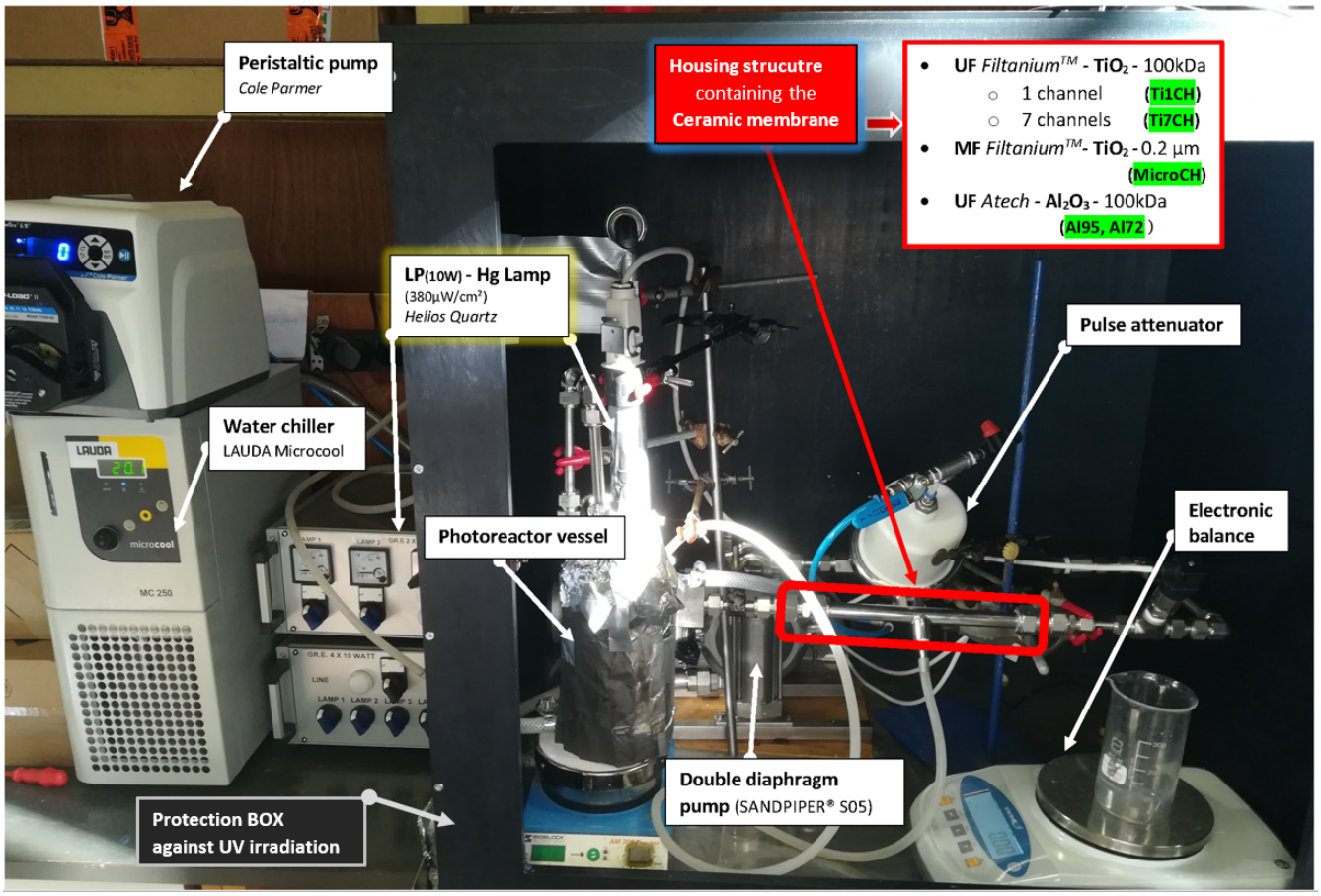

Figure 3.4: PMR experimental setup

3.2.1 General apparatus

The experimental setup of the photocatalytic membrane reactor module is presented above in Fig. 3.4. The setup is equipped with a two-liter cylindrical double jacket batch reactor vessel, connected to a cooling system (LAUDA MICROCOOL MC250) to maintain the reactor solution at constant temperature (~20±1 °C) during operation.

Centrally located in the vessel, a mercury low pressure UV lamp (HELIOS QUARTZ 10W, $\lambda_{max} = 254nm$; UV light intensity = 380 $\mu W/cm^2$) was used to irradiate the TiO_2 catalyst.

The feed solution was circulated in the closed loop circuit by an Air-Operated double diaphragm pump (P1-AODD) (Original ™ Series metal pump, WILDEN®Pump & Engineering).

A pulse dampener provided by the pump supplier was used to absorb the shock produced by the fluid pressure pulse generated by the pump. The shock was absorbed by injecting compressed air in a chamber behind the diaphragm, creating a pneumatic damper. This attenuator enabling the feed-flux detector to function properly was important to rigorously perform these experiments to avoid flux alteration throughout

the experimental tests.

In addition to this feed cross-flow velocity detector, two other sensors were used in order to continuously measure temperature and transmembrane pressure.

3.3 Experimental approach

A simplified scheme of the split-type PMR experimental setup (Fig.3.4) used to perform the experiments as well as the different steps (Fig.3.6) followed to perform a specific experiment are presented below.

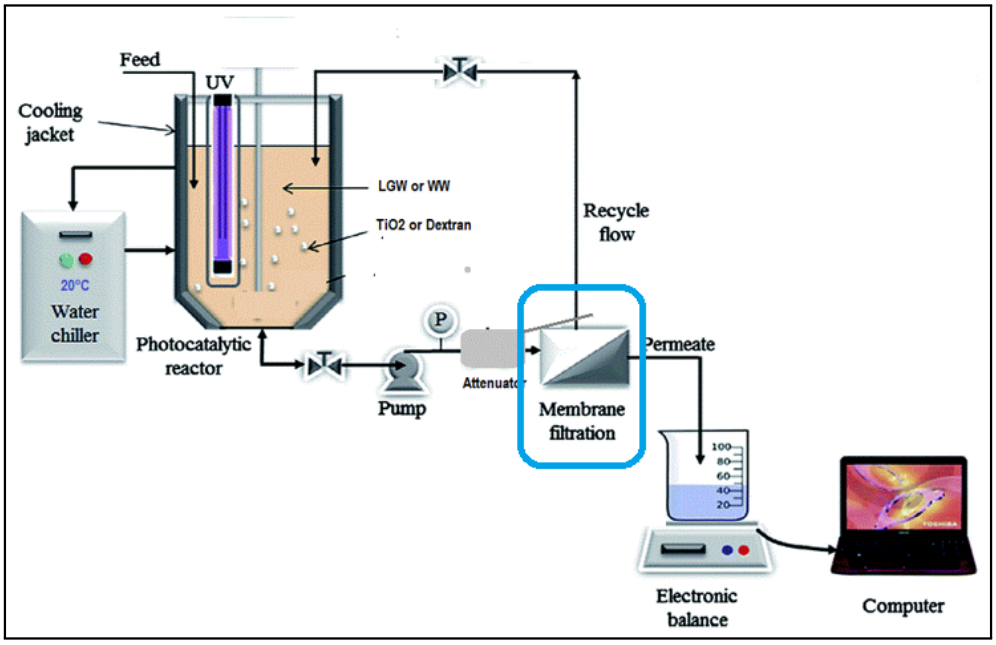

Figure 3.5: Simplified scheme of the experimental setup

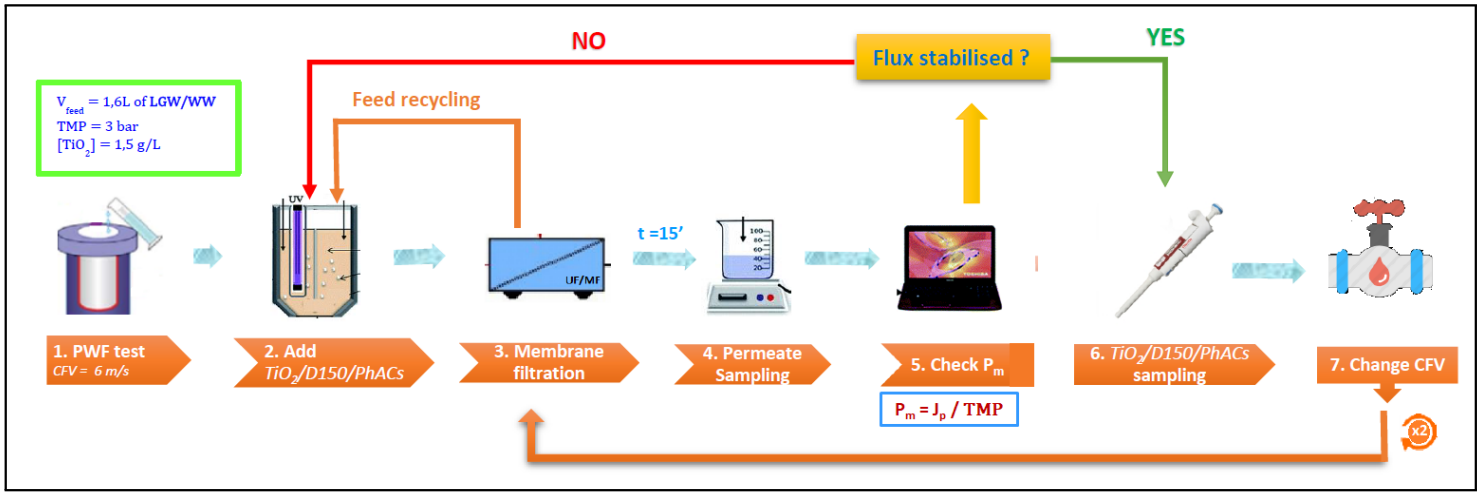

Figure 3.6: Global scheme of the different experimental procedures

3.3.1 Starting procedure

At the beginning of each experiment (STEP 1.), a feed solution of 1.6L of pure water (LGW) or wastewater (WW) was introduced into the reactor vessel and the cooling system activated to keep the solution at constant ambient temperature. After that, a rigorous starting procedure was initiated to get rid of all the air remaining/trapped in the closed circulating system. Air bubbles could affect the (ELNEO) flux detector's accuracy which is needed to accurately fix the initial cross-flow velocity at the rate required for the experiment. This procedure is detailed in the appendix C and consists of alternating low- and high pressure/flow conditions. The regulation of these two hydrodynamic parameters was done by adjusting respectively an allocated valve while looking at the pressure gauge (bar) and the digital flow detector (l/min) to control the specified working conditions (pressure and flow).

Throughout the experiments, the standard operating conditions can be defined : TMP = 3 bar, CFV = 3 m/s, T° = 20$\pm$1°C and TiO_2 loading = 1.5 g/L. For all experiments, the TMP was set at 3 bar while the CFV was case-specifically set at 1, 3 or 6 m/s. This change was achieved by adjusting the flow-valve on the delivery rate of the pump (STEP 7.).

3.3.2 Cleaning procedure

In order to remove the reversible and irreversible foulants stuck on/into the membrane, adequate cleaning methods have been used after each experiment. Identifying an adequate cleaning procedure was not an easy task as the chemical method suggested by the manufacturer did not work out. After investigations and testing, a three-stage procedure was established : first, the membrane was placed for 2 hours in an Series FP oven (BINDER) at 250°C in order to thermally degrade the organic matter (dextran) still present in the pores.

Afterwards, the catalyst cake layer was removed manually with a smooth cylindrical plastic rod to scrap the cake layer out of the membrane without damaging the membrane surface. Then the membrane was placed into an ultrasonic bath (FISHER SCIENTIFIC) during 20 min. This sonolysis step is used to break the aggregated catalyst particles and further degrade organic compounds trapped into the small pores of the membrane medium by means of the ultrasounds causing acoustic cavitation which creates local microzones of high temperature and pressure.

Finally, the chemical cleaning procedure of the manufacturer was adopted [46]. This last step removed the hydraulically irreversible fouling left by means of a cleaning agent which dissolves, displaces or chemically modifies the foulants or the fouling layer [37]. First an alkaline cleaning was performed using an aqueous solution of NaOH (15-20 g/L) at 85°C during 30 min to solubilize the organics. Then, the membrane was rinsed with LGW until it reached a neutral state and then placed into an acidic bath prepared with an aqueous solution of 75% H_3PO_4 (1 mL/L) at 50 °C for 15 min to remove the inorganic deposit.

3.4 Membrane characterisation

3.4.1 Permeability measurements

Following on from the starting procedure, the feed flowing in the lumen side of the membrane and the permeate were collected from the membrane outer shell (STEPS 3-4). The permeability of the membrane is key parameter and it is measured at different moments:

- After the starting procedure, the permeability is measured with LGW. This water step is held until the permeability is stabilised. Thereafter, the chemicals (TiO_2 photocatalyst or dextran) are added in the system at defined operating conditions
- After the addition of TiO_2 catalyst or dextran

The permeability test (STEP 4-5) is performed by measuring water or permeate flux flowing through the lumen side of the membrane to its outer part using a gravimetric method. The water/permeate is collected in a bucket on a scale (see STEP 4). The weight of water/permeate is continuously measured with the time. The weight is converted to volume using a density of 1 kg/dm^3 neglecting the change of density due to the addition of dextran/photocatalyst. The water permeate flux is then calculated (STEP 5) with following equation :

$$\boxed{J_m = \frac{\dot{V}_P}{A_m}} \qquad [dm^3/m^2/h] \tag{3.1}$$

where J_m is the permeate flux, A_m the membrane effective area [m^2] and $\dot{V}_P$ the volume flow [dm^3/h] calculated by the following equation :

$$\boxed{\dot{V}_P = \frac{m_w \cdot 120}{1000 \cdot \rho_w \cdot t_f}} \qquad [dm^3/h] \tag{3.2}$$

where m_w [g] is the mass of permeate measured during a t_f=30 sec filtration period, ρ_w is the water density = 1 [kg/L] in standard conditions, "1000" is the conversion factor for [g→kg] and "120" for converting [30s→h].

Finally, it was enabled to calculate the membrane permeability (P_m) as the flux per unit pressure differential across a membrane according to Darcy's law:

$$\boxed{P_m = \frac{J_m}{TMP}} \qquad [dm^3/m^2/h/bar] \tag{3.3}$$

Once a stable flux/permeability was achieved, a specific procedure developed for a target research question was followed.

3.4.2 Dextran rejection

The initial experiments used dextran from Leuconostoc spp.[2] with average molecular weight of 150 kDa (SIGMA-ALDRICH) as a model compound to evaluate the separation properties of the membranes. The concentration of the Dex150 sugar in the feed was set at 1 g/L. The rejection coefficient (R, %) was calculated on basis of the following equation:

$$\boxed{R(\%) = \frac{C_f - C_p}{C_f}} \tag{3.4}$$

where C_f (mg/L) and C_p (mg/L) represent the concentration of the model molecule i.e. dextran in this case, in the feed and permeate streams respectively. These concentrations were obtained by analysing the feed and permeate samples using ELSD which will be further introduced in 3.5.1.

3.4.3 Anti-cancer drugs (PhACs)

In this work, four cytostatic drugs obtained from SIGMA-ALDRICH were analysed :

Cytostatic compound	Abbre-viation	Formula	Cytotoxic class	Cancer treated	m/z ratio
5-Fluorouracile	5-FU	$C_4H_3FN_2O_2$	Antimetabolite	colon, esophagus, stom-ach, pancreas, breast and cervical	130
Capecitabine	Cap.	$C_{15}H_{22}FN_3O_6$	Antimetabolite	breast, stomach and colon	360
Cyclophosphamide	CP	$C_7H_{15}Cl_2N_2O_2P$	Alkalyting agent	lymphoma, leukemia, ovaries, breast, lung, neuroblastoma, and sarcoma	260
Ifosfamide	IFO	$C_7H_{15}Cl_2N_2O_2P$	Alkalyting agent	testes, sarcoma, bladder, lung, cervical, and ovaries	260

Table 3.2: Applications of cytostatic compounds studied and their respecitve mass-to-charge ratio (used for detection by MS) [18], [19]

[2]Gram-positive lactic acid bacteria used for the fermentation process of sugar into lactic acid

These drugs are model cytostatic compounds commonly used for laboratory degradation tests because of their stability [41].

The rejection of these pharmaceuticals was calculated using equation 3.4 and the concentration values were obtained by means of UPLC/MS which will be introduced in the next section.

Safety precautions

These anti-cancer drugs used in the lab must be cautiously treated as they are highly toxic and hazardous in case of skin or eye contact (irritant) [47]. Besides, when operating in PMR conditions, the UV irradiation field was reduced by encapsulating the whole setup in a black protection box as shown in Fig. 3.4 and the box door was closed when UV light was switched ON. Other additional safety equipments were used in order to avoid any direct contact with the chemicals and the UV-light :

- safety glasses and face shields for eye protection
- regular change of latex gloves for hands protection
- full body protective suit

3.5 Analytical methods

Three different techniques were used to analyse the samples by measuring the concentration of the chemical compounds of interest: 1) Evaporative Light Scattering Detector (ELSD) 2) Ultra Performance Liquid Chromatography coupled with Mass Spectrometry (UPLC/MS) and 3) Spectrophotometry.
The ELSD and UPLC/MS techniques were used to respectively measure the concentration of dextrans and PhACs in the feed and/or permeate. The ELSD and UPLC analysis were done using an Agilent 1200 series apparatus.

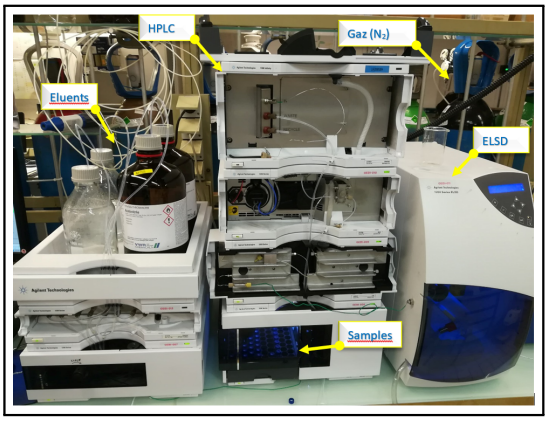

Figure 3.7: ELSD apparatus in GEBI UCL lab

Figure 3.8: Spectrophotometer model as in iMAP UCL lab [11]

Calibration curves

These analytical methods do not directly provide a result in form of concentration of the target compound present in the samples but rather an area/absorbance response of the standard solution for each peak related compound. Therefore, to convert this area underneath the peaks (*ELSD and UPLC*) or absorbance (*spectrophotometry*) to concentration values, one need to determine calibration curves for each analyte. This was done by running analyses of a compound at different well-known concentrations (200, 100, 50, 20 and 10 ppm). Throughout the experiments, the calibration curves of Dex150 and TiO_2 have been established and are available in the appendix D.

3.5.1 ELSD for Dextran analysis

The ELSD is a concentration detector which consists of a three stage process as shown in Fig. 3.9: the nebulization of the eluent into a steady flow of inert gas. This aerosol passes through an evaporation chamber where the solvent is removed from the solution and finally, by means of a photodiode and a laser beam, the irradiated non-volatile particles deflect the scattering light and this deviation is detected by the photosensitive device. The signal depends on the molecular mass of the solute. ELSD allows to perform carbohydrate separations by gradient elution from organic eluents. The mobile phase used was an organic mixture of two solvents methanol/water in the following proportions: 20/80%.

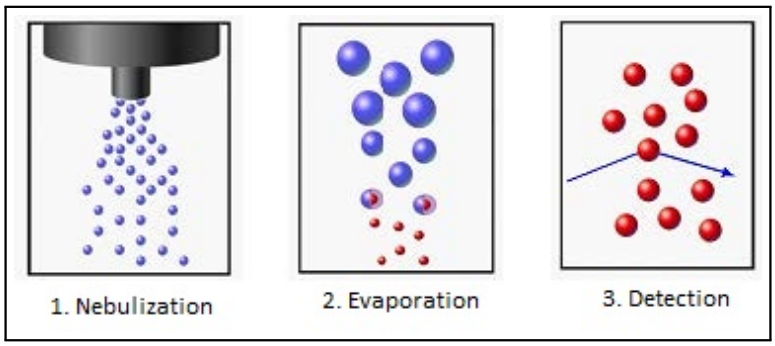

Figure 3.9: ELSD Principles of Operation [12]

3.5.2 UPLC/MS for PhACs analysis

This UPLC configuration was performed through an Agilent 6100 triple quadrupole LC/MS apparatus. It is worth noting that UPLC is quite similar to HPLC except that UPLC operates at higher pressure (1000 bar) compared to HPLC (400 bar) which allows finer particles to be used to fill the column and more precise measurement.

Technically, $5\mu L$ from the sample vial were extracted and pumped passing though an elution column (HSS5). The eluent consists of a mixture of two organic solvents : a pure (100%) CH_3CN solvent and 95/5%

H_2O/CH_3CN solution. The limit of detection (LoD) and limit of quantitation (LoQ) of the instrument are respectively 3 and 10 ppb[3]. The LoD is the lowest concentration at which the instrument can detect an element whereas the LoQ corresponds to the lowest concentration that can be determined by the instrument with an acceptable level of repeatability precision [48]. The global analytic procedure is shown in the figure below. The MS was able to detect the four PhACs based on their retention time in the column by means of their respective mass-to-charge ratios (m/z) which are reported in table 3.2. The higher this ratio, the more time is needed for the compound to pass through the separation column.

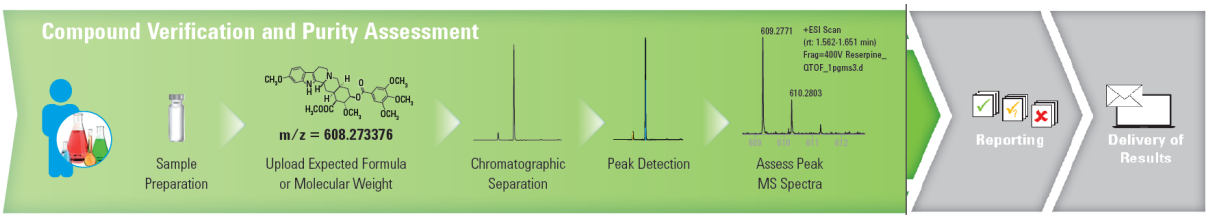

Figure 3.10: UPLC/MS principles of operation. Figure modified from [13]

3.5.3 Spectrophotometry

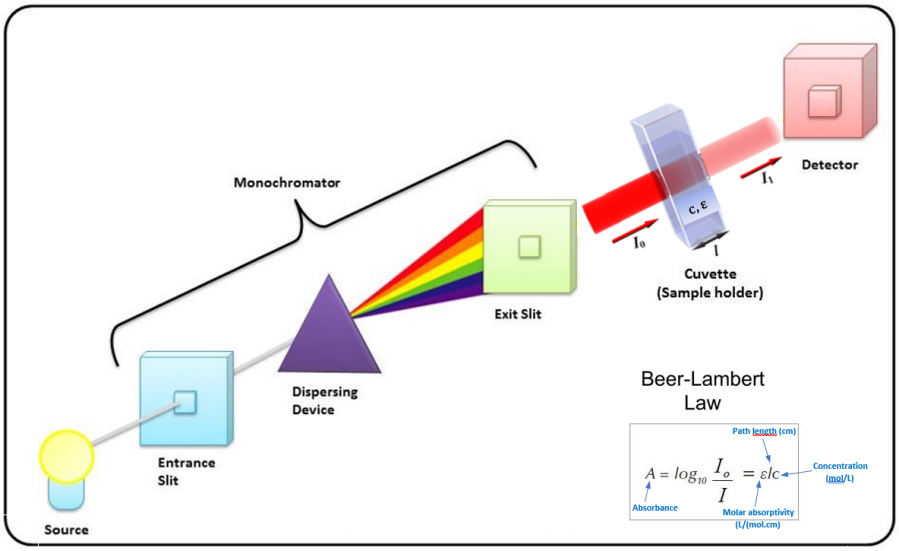

Figure 3.11: Representative diagram of UV-vis spectrophotometer principle

Catalyst concentrations were measured using a DR/400 UV-vis HACH® spectrophotometer in order to determine the concentration of photocatalyst in the feed after a certain elapsed time according to the mechanism procedure shown in Fig. 3.11 [11]. The main working principle of spectrophotometry consists in measuring the absorbance (A) of light using Lamber-Beer's law expressing the linear relationship

[3] Statistically, LoD = 3*SD and LoQ = 10*SD of the limit of blank (LoB) which corresponds to the highest apparent concentration expected by replication of blank sample measurements

between absorbance and concentration (C) of a compound at a fixed wavelength. The 1 mL samples were diluted 10 times with LGW before analysis because an inital concentration of 1g/L would saturate the spectrophotometer. As the maximum peak of absorption for TiO_2 was experimentally determined to be at λ_{max}= 390 nm, a linear calibration curve was used to convert the absorbance into $[TiO_2]_{diluted}$ by means of the Lamber-Beer's law (see appendix D.3). Finally, the real concentration was obtained multiplying the latter by a factor of 10. For this instrument, the LoD = 0.002 g/L and the LoQ = 0.006 g/L.

Chapter 4

Results and discussion

4.1 Membrane characterisation

The membranes were first characterised by performing LGW permeability tests following the procedure described in 3.4.1 and which consists in measuring the pure water flux flowing through the membrane shell during a pre-fixed time period. This flux is further converted into membrane permeability by using Darcy's law. The experiment was carried out for 1h and the results are shown in Fig. 4.1. Later in this section, these permeability values will be used to determine the intrinsic membrane resistance.

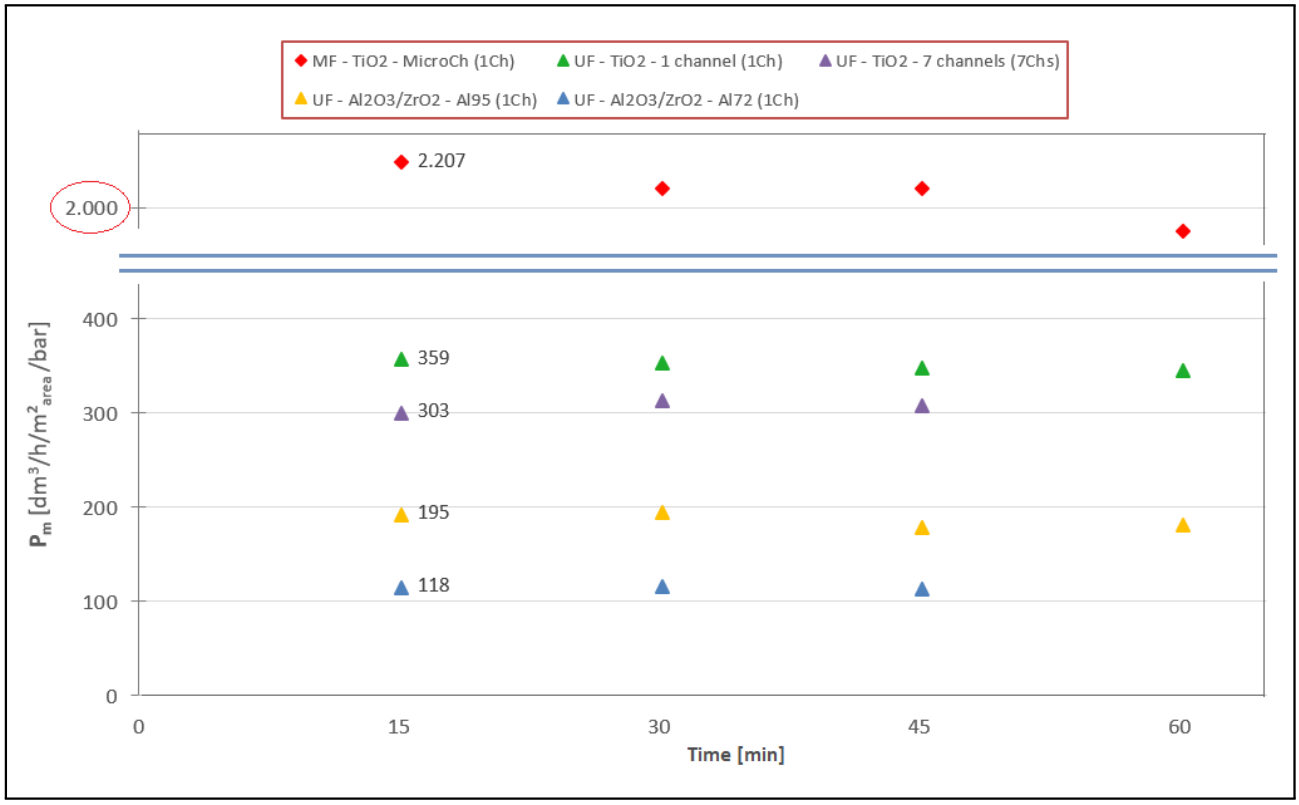

Figure 4.1: Changes of membrane permeability during UF (100kDa) and MF (0,2μm) of pure water through Al_2O_3/ZrO_2 *(1 channel)* and TiO_2 *(1 and 7 channels)* ceramic membranes (process parameters : TMP = 3 bar, CFV = 3 m/s)

In the case of UF membranes, Fig. 4.1 indicates that no drastic changes of permeability were happening after the one hour period as the permeability stabilized. *Mozia et al.*[9] found that for 100kDa UF-TiO_2 membranes, their permeability continuously decreased over time, especially over the first 12h of the experiment reaching a value of ca. 170 [$dm^3/m^2/h/bar$] as shown in figure 1.10a. According to the authors, this decline was related to the wetting of the membrane surface and pores. Indeed the authors evidenced that membranes kept dry showed higher permeate flux regarding hydrated ones, hence causing a permeability decrease over time until stabilisation. The membranes in this study were already hydrated before starting the experiments, and therefore no permeability decrease was observed.
Also of note is the significant difference between the initial permeability of the TiO_2 and Al_2O_3 membranes. This can be explained by the fact that titania membranes are intrinsically more hydrophilic compared to alumina membranes [49]. Hence, it is easier for water to pass through the pores of the titania one.

Besides, one can notice a significant deviation in permeability in LGW conditions between the UF-Al72 ($P_m = 117\ dm^3/m^2/h/bar$) and UF-Al95 ($P_{m-av} = 192\ dm^3/m^2/h/bar$) membranes although these membranes are identical (provided by the same manufacturer). This discrepancy can be explained by the fact that those are cheap ceramic membranes presenting a wide pore distribution which is not well defined as shown in Fig. 1.5.

Membrane cleaning

After each test, the membranes were thoroughly cleaned following the 3-steps procedure described in 3.3.2. As mentioned in that section, the development of this final procedure resulted from a trial-and-error methodology by alternately fouling the membrane with dextran and afterwards applying a trial cleaning procedure until recovering permeability values close to LGW. The different trial steps are shown on Fig. E.1 in appendix.

4.2 Study of the influence of hydrodynamic conditions on membrane fouling

4.2.1 Study of the effect of cross-flow velocity

Procedure

In order to study the influence of cross-flow velocity on the reduction in UF and MF membrane permeability (Al95, TiO_2-1Ch and TiO_2-7Chs), a 4h experiment was performed as per the following procedure: first, a LGW permeability test was performed on ceramic membranes at a constant TMP of 3 bar until the permeate flux stabilised at a given CFV. The corresponding pure water flux permeability values are presented as dashed horizontal lines in Figs. 4.2 and 4.5.

Then, a TiO_2 photocatalyst (1.5g/L) was added and a UV lamp activated in order to work in prevailing PMRs conditions. From then on until the end of the experiment, membrane permeability was evaluated every 15 min using the gravimetric method described in 3.4.1. This procedure was conducted at CFVs of 6, 3 and 1 m/s, in this order. The changes in UF and MF membrane permeability over time are shown in Figs. 4.2 and 4.5 respectively.

Influence for UF membranes

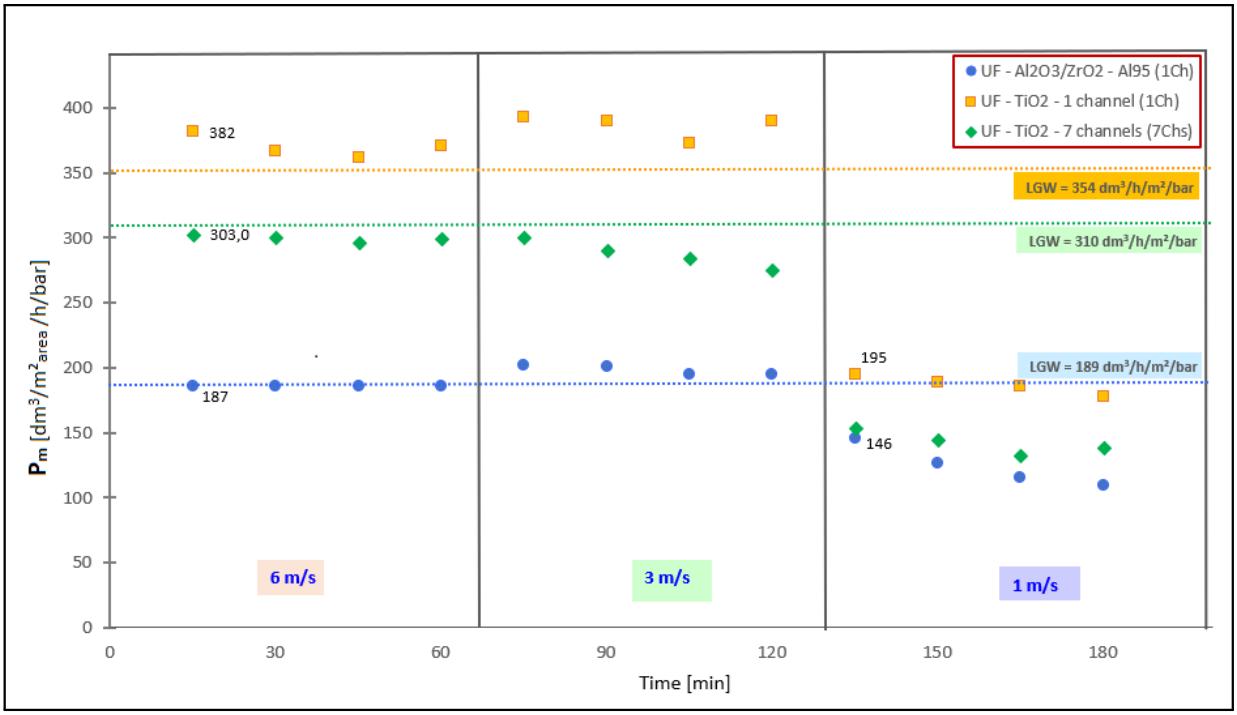

Figure 4.2: Influence of feed cross-flow velocity on the membrane permeability of 1 and 7 channels UF (100kDa) membranes (process parameters : TMP = 3 bar, 1.5 g/L TiO_2)

For UF membranes, one can see in Fig. 4.2 that during the experiment, no significant change in permeability was observed until reaching the 1 m/s flow condition. Indeed, for all UF membranes, no decrease in membrane permeability occurred at 6 and 3 m/s after adding a catalyst. Globally, the membrane performance was not altered at these higher flow velocities. This could be explained by the fact that no fouling took place under these operating conditions. These results are similar to the one found by *Mozia et al.* on 100kDa UF membranes.

However at low cross-flow velocity (1 m/s), the permeance of the membranes drops significantly and this fall can be correlated with the development of a catalyst cake layer at the membrane surface. It is known that the deposition of particulates on the membrane surface results from the balance between two normal forces acting on the particles as illustrated in Fig. 4.3. These include the lift force (F_L) induced by the turbulent stream in the membrane channel and the drag force of the permeate flow (F_Y). As the CFV was

decreased, the lift force was gradually overwhelmed by the drag force of the permeate [50]. As a result, catalytic particles started to deposit on the membrane surface. After deposition, an additional adhesive force (F_A) caused by interaction of the particle with the membrane surface comes into play [14]. The balance between this adhesion and the lift force will determine whether or not this particle goes back into the bulk stream. In the case of highly turbulent flow regimes (Re»2300) inside the membrane channel, particles would not last long onto the membrane surface as the lift force would overcome the adhesive force exerted by the membrane surface [41], [50].

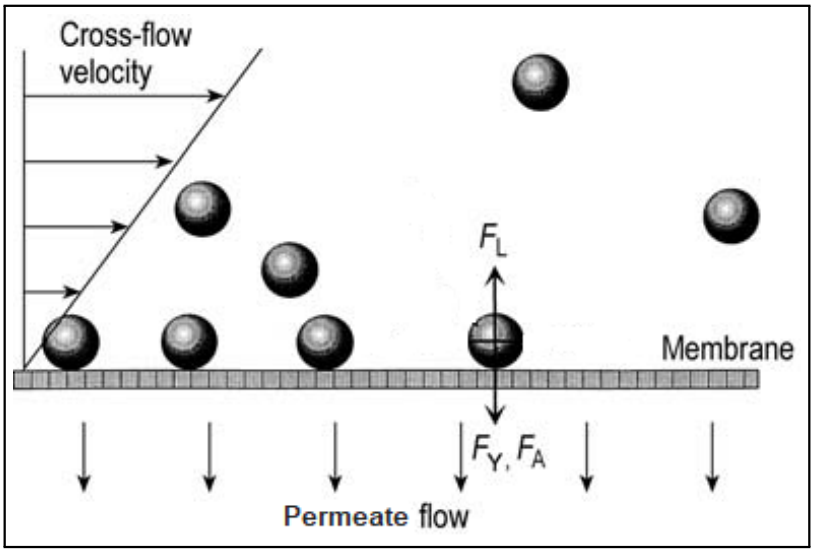

Figure 4.3: Scheme of the different normal forces which play a role in particle deposition for cross-flow filtration: F_L = hydrodynamic lift force; F_Y = drag from the permeate flow; F_A = adhesion to the membrane. Figure modified from [14].

In order to verify this hypothesis, feed samples taken after PMR operation at each CFV were analysed by spectrophotometry to evaluate the amount of catalyst remaining in the bulk stream. The results are presented in Fig. 4.4. These results are consistent with the assumption that the catalytic concentration drops by 50 and 63% at 1 m/s compared to 3 m/s values for the 1Ch and 7Chs membranes respectively. Moreover, compared to the initial feed concentration, respectively 65 and 73% of the catalyst was missing from the bulk flow. It was observed during membrane cleaning that this «missing» catalyst was concentrated onto the membrane filtration area (cake layer) and into the membrane pores.

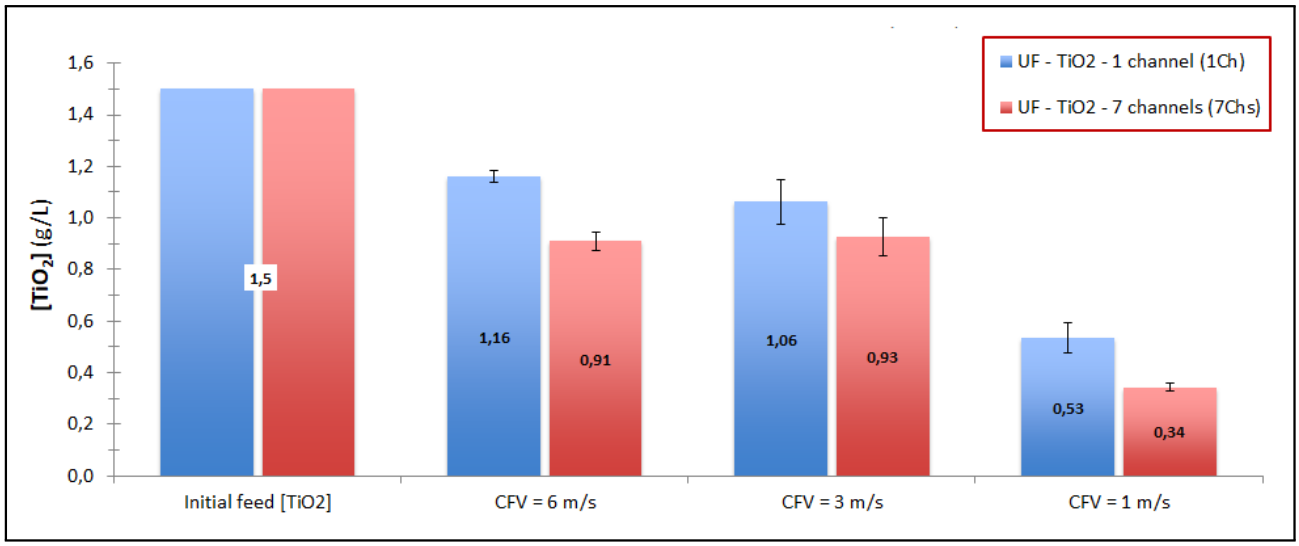

Figure 4.4: Influence of feed cross-flow velocity on [TiO_2] in the feed through Filtanium 100kDa UF membranes (process parameters : TMP = 3 bar, 1.5 g/L TiO_2)

Additionally, to check the highly turbulent flow regime assumption, the Reynolds numbers for the different membranes were calculated and are presented in table 4.1. A turbulence scale (high, moderate and low) was established by *Russo et al.* [51] in which they classified turbulent regimes by calculating turbulent intensity based on their Reynolds number. Following their procedure, *highly turbulent* flow regimes were calculated to occur at 6 and 3 m/s for the 1 channel configuration whereas all the other turbulent regimes are considered as *moderately turbulent*. Besides these turbulent regimes, a laminar flow regime exists for the UF-7Chs membrane at 1 m/s. These laminar flow conditions should enhance particles deposition and hence cause a more severe permeability decline compared to the 1 channel membrane. However, in Fig.4.2 the difference in permeabilities at 1 m/s between the two membranes remains the same for 3 and 6 m/s. This could be explained by the fact that the flow regime is close to the transition towards turbulence (Re > 2300) [52].

Membrane	$d_{channel}$ (mm)	**Reynolds number (-)**			**Flow regime**		
Cross-flow velocity	-	6 m/s	3 m/s	1 m/s	6 m/s	3 m/s	1 m/s
UF/MF- 1 channel	6	36.000	18.000	6.000	Turbulent	Turbulent	Turbulent
UF- 7 channels	2	12.000	6.000	2.000	Turbulent	Turbulent	Laminar

Table 4.1: Fluid dynamics in tubular membranes : TiO_2-Al_2O_3/ZrO_2 : 1 channel and 7 channels

Coming back to Fig. 4.2, the permeability falls from 187 to 146 $[dm^3/m^2/h/bar]$ ($\sim 20\% \searrow$) for the alumina membrane (Al95) whereas for its titania counterpart (TiO_2-1Ch), a more drastic decline from 382 to 195 $[dm^3/m^2/h/bar]$ ($\sim 50\% \searrow$) can be observed. This flux decrease could be explained by the fact that in both cases, a TiO_2 cake layer suddenly forms at 1 m/s on the membrane surface and hence the beneficial hydrophilic effect of titania applies to both membranes [2]. Indeed, since the fouling layer is blocking the access of the particles to the pores, the resistance to water flow due to pore blocking becomes negligible compared to the cake resistance and this thin cake layer constitutes the main resistance against filtration flow.

Simply put, the TiO_2 cake layer formed at the surface of both types of ceramic membranes ended being the only significant resistance to filtration flow as also observed by *Lee et al.* [43]. Furthermore, the permeability drop was less severe for the alumina membrane since its surface gained hydrophilicity due to the superhydrophilic TiO_2 particles contained in the cake layer.

Looking now at the two different titania membrane configurations (green and yellow), a similar cake layer formation was observed for both membranes (1Ch and 7Chs), indicating that more compact membranes react the same way as less compact ones towards membrane fouling.

To wrap up, the results revealed that for UF membranes, a sudden drop of permeability was observed at 1 m/s irrespective of the type of membrane which was caused by membrane fouling. This fouling has been observed in previous work related to the deposition of the catalytic particles on the membrane surface causing the development of a porous cake layer [9].

Influence for MF membrane

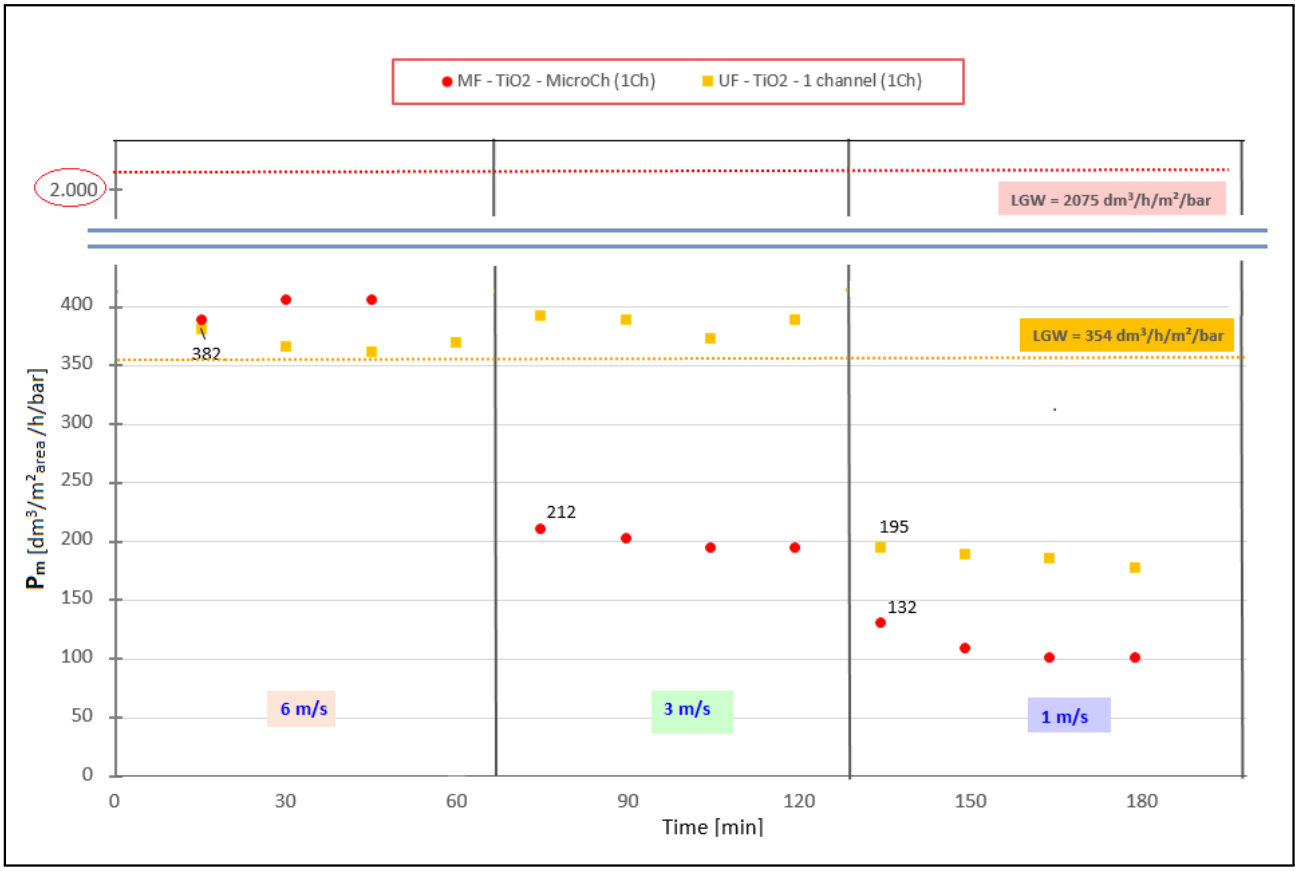

Figure 4.5: Influence of feed cross-flow velocity on membrane permeability of 1 channel MF (0,2μm) and UF (100kDa) membranes (process parameters : TMP = 3 bar, 1.5 g/L TiO_2)

For the MF membrane, the permeability values at 6 m/s were much lower than the LGW ones, which is inconsistent with the results *Mozia et al.* [9] found, working in the same conditions. Indeed, that study evidenced a positive effect of catalytic filtration by UF and MF at high cross-flow velocities, evidenced by much higher permeability values ($\sim 25\% \nearrow$) compared to LGW. They attributed that to the abrasion of the membrane surface by the catalyst particles due to shear forces induced at high cross-flow velocity.
In this case, the data shows no increase of permeability for the MF membrane, which suggests that the membrane had not been scoured by the catalyst particles but rather that they were already deposited into the pores and/or on the membrane surface. Another explanation could be that since the MF membrane already has large pores, their further enlargement by mechanical abrasion would have no significant impact on the membrane permeability. Although the turbulent flow conditions at high CFV would prevent stable deposition of photocatalyst particles onto the cake layer [50]. In brief, the supposition is that for MF, at 6 m/s the particles manage to penetrate into the large micropores and hence causing a substantial permeability decline.

During PMR operation, different results were obtained in the case of the MF membrane with respect to UF. Indeed, a significant drop was also observed but this time already at 3 m/s and an additional step-decrease occurred at 1 m/s. At 3 m/s, the permeability for the MF dropped in the same range as the UF at 1 m/s. The cause of this fall is the same as for UF membranes which is discussed above. At first sight this similarity could seem surprising since this membrane had larger pores compared to the UF ones, hence one might think that pore blockage would be more inclined to take place as the pore size ($0.2\mu m$) is larger than the photocatalyst particles (ca. 21 nm [2]). But actually, these particles exhibit a wide particle size distribution and once they have been dispersed into the liquid feed, they can reach a hydrodynamic size about 300nm, much larger than their primary size [53]. Furthermore, the particles start aggregating to form larger agglomerates reaching an average size of ca. $4.2\mu m$, which can be effectively rejected by the MF and UF membranes [9].

Effect of flow turbulence

In the continuity of the work performed by *Mozia et al.* [9] regarding the danger of pore blockage by TiO_2 particles, the effect of enhanced turbulent flow conditions on MF was investigated. To do so, a permeability test was performed by working under the same operating conditions as before (TMP = 3 bar, 1,5 g/L TiO_2), by alternately switching OFF and ON the pulse dampener, hence promoting turbulence in the flow for the OFF-mode when the attenuator was not working.

By working under these operating conditions, it would be expected that this additional turbulence inside the membrane channel would enhance the membrane permeance by minimizing the formation of a laminar cake layer. However, the results, available in the appendix E.3, say otherwise. Indeed, although the turbulent regime was enhanced, there is no notable effect of this dampener on the membrane fouling since there was no difference of permeability whether the attenuator was switched ON or OFF. Consequently, one could conclude by looking at the values for Reynolds number with application of the pulse dampener (see table 4.1), that since these values already characterise a high turbulent flow regime, the additional turbulence provided by the dampener seems unremarkable.

4.2.2 Study of the effect of water matrices (Al95, TiO_2-1Ch)

After performing tests using demineralized water, similar experiments to those conducted previously but performed however this time with wastewater (its composition is given in subsection 3.1.1) in order to investigate the impact of the latter on the membrane fouling. To this end, the UV lamp was switched off in order to avoid the degradation of the NOM present in the wastewater as to not mitigate the organic fouling process. One would expect, as suggested by *Zhang et al.* [2], that the use of this water would enhance the hydraulic membrane resistance against filtration flux. This fouling rise, according to *Zhang et al.*, would result from the adsorption of organic material present in the wastewater (mainly in the form of dissolved organic matter) onto the catalyst particles which could further penetrate the cake layer and cross-link the cake structure leading to a denser fouling layer. Besides, these organic particulates could also enhance pore blocking depending on the size of organic matter.

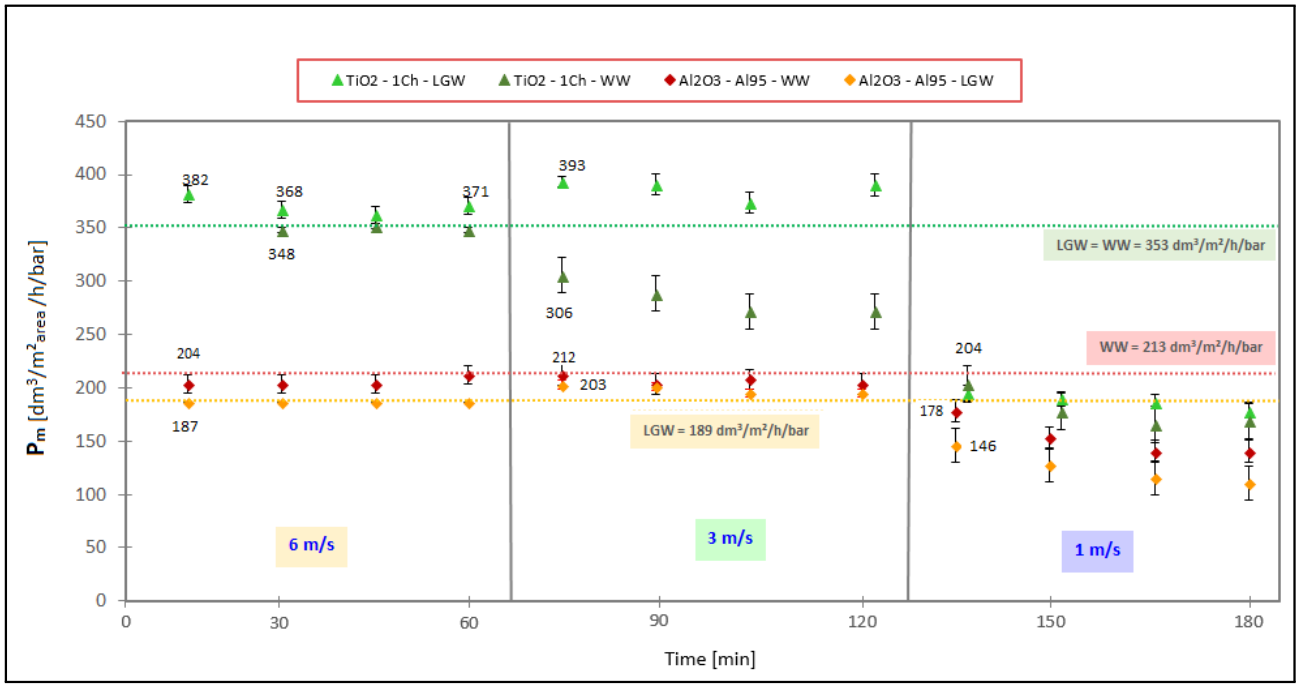

Figure 4.6: Influence of water matrices on membrane permeability of 1 channel alumina (*Al95*) and titania (*TiO_2-1Ch*) UF (100kDa) membranes (process parameters : TMP = 3 bar, 1.5 g/L TiO_2)

Results obtained are shown in Fig. 4.6 for the monochannel alumina and titania UF membranes. According to this figure, the results indicated no significant changes by using wastewater. The permeability values for wastewater in the case of the alumina membrane were slightly higher compared to LGW corresponding respectively to 221 and 195 $[dm^3/m^2/h/bar]$. However, this discrepancy was not considered significant. Regarding the TiO_2-1Ch membrane, the trend is the same as LGW till transition to 3 m/s. Indeed, at this CFV the permeability starts to gradually decrease from 306 before stabilizing at 260 $[dm^3/m^2/h/bar]$ while for LGW the permeability remained constant at ca. 387 $[dm^3/m^2/h/bar]$. However, what happens next is even more interesting when passing to 1 m/s, the permeability for both water matrices merge afterwards at

ca. 200 $[dm^3/m^2/h/bar]$. To gain a better overview of the situation, the data were converted in terms of hydraulic resistances and plotted in Fig. 4.7.

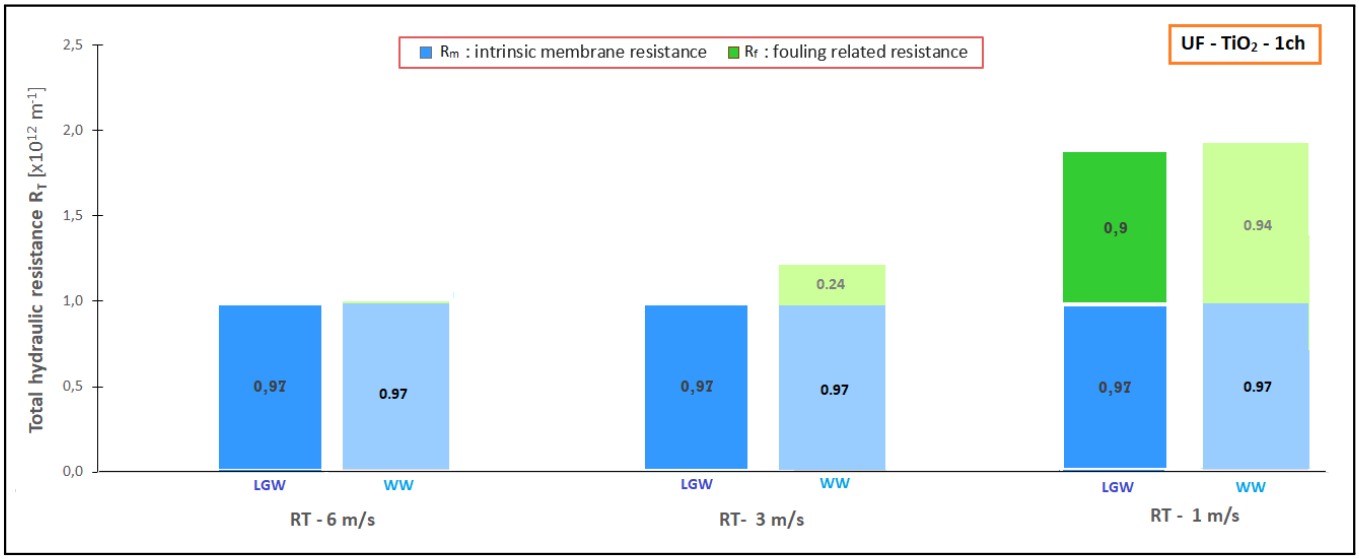

Figure 4.7: Influence of water matrices on fouling phenomena (R_m, R_f & R_T) for 1 channel TiO_2 UF (100kDa) membrane (process parameters : TMP = 3 bar, 1.5 g/L TiO_2)

For both water conditions, the membrane resistance (R_m) are equivalent which suggests that without using catalyst particles, no evidence of additional fouling related to potential organic matter was noticed. However, one can see a significant change for the fouling resistance (R_f) at 3 m/s as it was previously shown, although the resistance due to fouling are equivalent in the two water matrices at 1 m/s ($R_T \approx$ 2E+12 m^{-1}). One possible explanation would be that at 3 m/s, the little amount of organic material left (0.5 mg/L of BOD_5, see table 3.1) would either cause pore blocking fouling (as previously explained) or get attached to the membrane surface and hence decrease its hydrophilic properties. This last phenomenon assumes that the organic particles are mainly hydrophobic, which is plausible as 50% of organic matter in wastewater constitutes proteins which are a combination of hydrophilic and hydrophobic compounds [54]. As previously stated, the cake layer constitutes the main contribution to the overall fouling resistance. And following the foregoing reasoning of fouling at 3 m/s, the lack of overall resistance growth at 1 m/s for wastewater can be evidenced by the fact that the amount of organic material present is very low (0,5 mg/L) compared to the amount of catalyst involved (1,5 g/L). As it is known that the hydrophilic titania particles swiftly deposit on the membrane boundary, the small hydrophobic effect induced by the organic material would immediately be counterweighted.

4.3 Study of the influence of TiO_2 cake layer formation on PhACs and dextran rejection

After looking at the conditions promoting a cake layer formation for UF membranes (CFV = 1m/s), an interesting question emerged : what if this photocatalyst cake layer would help filter PhACs ?
To verify this hypothesis, a similar procedure to that of RQ1 was used except that a mixture of PhACs were initially added before the addition of the TiO_2 photocatalyst. Since it was observed in Fig. 4.2 that the membrane permeability remained stable in the 6-3 m/s range and that the cake layer formed at a cross-flow velocity of 1 m/s, this current experiment was conducted at fluid velocities of 6 and 1 m/s. At each flow condition, the rejection of PhACs in presence of TiO_2 were determined as well as the Dex150 rejection to see if the developed cake layer would help filter the smaller (organic) particles as suggested by *Mozia et al.* [32]. The results are shown in Fig. 4.8.

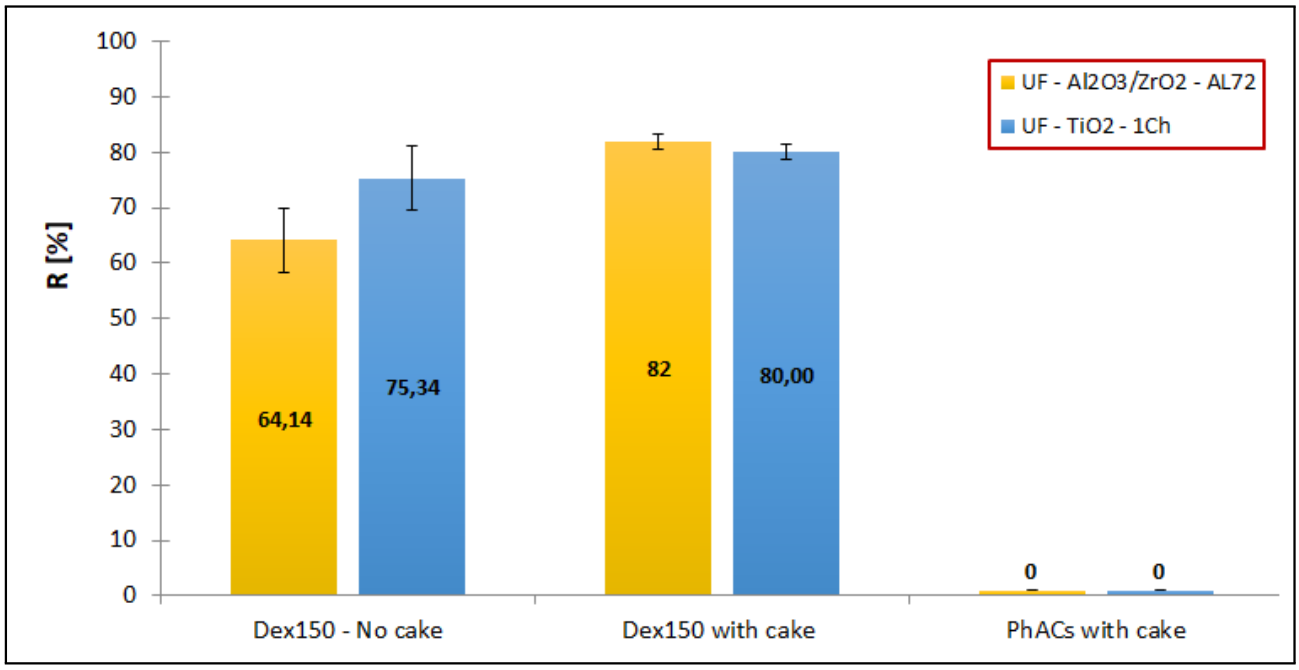

Figure 4.8: Rejection of dextran (150kDa) and PhACs with/without presence of cake layer of 1 channel alummina and titania UF (100kDa) membranes (process parameters : TMP = 3 bar, 1.5 g/L TiO_2)

Both membranes tested showed an increase of dextran rejection in presence of a cake layer. For the alumina membrane, the dextran rejection increased by respectively ca. 30% and 7% in the presence of the cake layer for alummina and titania membranes compared to LGW. According to [9], [32] and [8], this rejection growth was justified by the formation of a dense cake layer (so called "secondary dynamic membrane" - see Fig. 1.12) by the large TiO_2 particles on the membrane surface which improved the rejection of smaller particles i.e. dextran.

However, no rejection of anti-cancer drugs were observed for both UF membranes. This suggests that the porosity of this additional filtration cake layer allowed the smaller PhACs to pass through and therefore, no rejection took place. The ease with which PhACs passed through the membrane could be additionally supported by the investigations of *Ganiyu et al.* [39] presented in 1.5. These authors evidenced that UF was not suitable to separate small molecular weight compounds.

In conclusion, the additional catalyst cake layer formed during PMR operation has shown to be totally ineffective at removing tiny cytostatic drugs (<400 Da [40]) although it enhanced the membrane selectivity towards small organic compounds.

4.4 Study of the membrane stability regarding separation properties over long-term operation

Procedure

In line with the first presented approach and with the initiated work towards stability of ceramic membranes during PMR operation by *Mozia et al.* [9], a procedure to further investigate the change of separation properties of an UF membrane (MWCO = 100 kDa) caused by the mechanical abrasion of the photocatalyic particles was established. Regarding the operating conditions, a quite similar methodological approach to *Mozia et al.* [9] was applied but operating in this case at higher flow velocity of 6 m/s in order to promote the risk of damaging the membrane surface by photocatalytic particles.

It is worth noting that a bigger dextran of 150 kDa instead of 70 or 110 kDa as in the reference paper [9] was used. This results from the fact that when performing pure water rejection tests in absence of TiO_2 for Dex110 without adding any chemical compound (catalyst or PhAC), the values were very low (<35% - see appendix E.2) compared to the high values found by *Mozia et al.* (up to 99%). This could be explained either by the asymmetrical porosity distribution across the different layers constituting the membrane filtration shell or another plausible justification is the wide particle size distribution of the dextran.

In this study the rejection coefficient determined at the beginning of the experiment (t = 0 [h]), without the presence of photocatalyst, served as a point of reference during the assessment of the degree of the membranes' damage by the abrasive action of the TiO_2 particles. The results are summarised in Fig. 4.9.

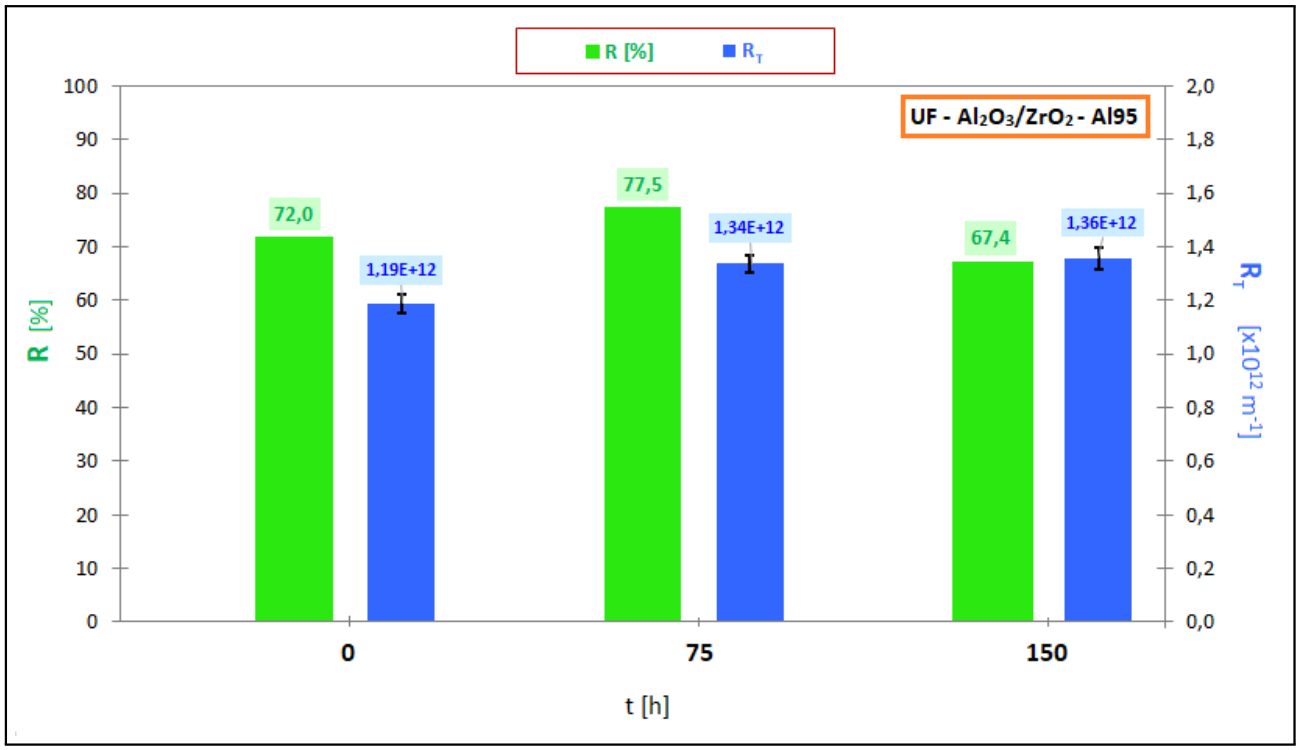

Figure 4.9: Changes of separation properties of 1 channel alumina (Al95) UF (100kDa) membrane during PMR operation (process parameters : CFV = 6 m/s, TMP = 3 bar, 1.5 g/L TiO_2)

Discussion

Compared to the values found in LGW conditions (t=0), rejection values (R%) after membrane cleaning show an increasing trend of ca. 10% after 75h and reversely, after 150h, a dip of 10% was observed. These small fluctuations were not regarded to be significant as the membrane resistance remained constant throughout the whole experiment. Therefore, the small decline after 150h with respect to 75h, was considered insignificant. In order to make this supposition, the total hydraulic resistances were calculated using the permeability values determined at each step of the process (0, 75 and 150h) following the standard procedure 3.4.1. By operating at high cross-flow velocity, the fouling contribution to the overall hydraulic resistance (R_T) was considered as insignificant ($R_f \approx 0$). Therefore, the only contribution against the filtration flux constitutes the intrinsic membrane resistance (R_m). In contrast to the rejection values, the same R_m level was maintained after 75h and 150h. Indeed, if the rejection drop was caused by to the loss of separation properties due to the scouring effect by the TiO_2 catalyst particles during the final step (150h), one would have expected R_m to follow the rejection fall.

Besides it can be noticed that the membrane resistance obtained for the alumina membrane (1,19E+12) is quite higher compared to the one for UF titania membrane (0,97E+12) illustrated in Fig. 4.7. This is consistent with the permeability values observed in Fig. 4.1 as R_m is inversely proportional to P_m according to equation 1.6.

As a conclusion, the alumina UF membrane did not suffer from separation layer damage after a long time of operation as its separation properties (R%) were not altered. This is consistent with the observations made by *Mozia* [9] and *Szymanksi* [10] after 100h of operation for their TiO_2 100 kDa UF membrane whose results are shown in Figs. 1.11a and 1.11b .

Conclusions

This master thesis is part of an overall wastewater treatment project involving slurry Photocatalytic Membrane Reactors (PMRs) as a promising water purification technology. As introduced in the literature survey, this hybrid system combines the high degradation rates obtained with suspended photocatalyst and the membrane separation properties as a way to continuously recycle these photocatalyst particles inside the system. Nowadays, the scientific community is investigating different ways to enhance the performance of this technology and one of them is to improve the rejection and stability of the membrane module towards photocatalytic particles. Ceramic membranes appeared to be consistent with these criteria as these membranes have shown to be robust and fouling tolerant. However, this robustness and fouling tolerance still need further development on their inability to reject small molecular weight compounds (e.g. pharmaceutical active compounds (PhACs)).
The objective of this study was to determine 1) the effect of hydrodynamics and water matrices on membrane fouling, 2) how the fouling cake layer could positively contribute for the filtration of small contaminants, and 3) how the stability of a ceramic membrane would be affected on long-term operation.

Experiments realised under flow conditions prevailing fouling by TiO_2 photocatalytic particles, in the case of Al_2O_3/ZrO_2 and TiO_2 ultrafiltration (UF) membranes, have shown that above 3 m/s no effect of feed cross-flow velocity (CFV) on the membrane permeability was found. This was consistent with the observations made by *Mozia et al.* [9] for the same experimental conditions and membrane properties. However, below 3 m/s the formation of a catalyst cake layer took place, witnessed by a drastic decline in the membrane permeation which was in agreement with literature. This fall was attributed to membrane fouling and was evidenced by measuring the catalyst concentration in the feed: a decline of this concentration confirms the accumulation of catalyst on the membrane surface and/or into the membrane pores.

In case of microfiltration (MF) membrane, a drastic drop in permeability during PMR operation was already found at 3 m/s instead of 1 m/s for UF membranes. Besides, at 6 m/s the MF showed a drastic drop in permeability below the values measured for pure water. This was attributed to the larger pores of MF membrane wherein the finest particles of catalyst can enter and stay blocked due to pore configuration and interaction with membrane material.

As a conclusion, to avoid deposition of the TiO_2 on the membrane and to keep a good permeability, the UF membrane must operate at a CFV higher than 3 m/s in order to effectively reject the catalytic particles and to keep a good permeability without hindering effect of membrane fouling on transmembrane flux. For MF membranes, optimal rejection efficiency is achieved for CFV higher than 6 m/s.

Besides, the type of membrane material and configuration on the membrane permeation were found to be

insignificant. The hydrophilic advantage of titania over alumina UF ceramic membranes became meaningless as a hydrophilic cake layer surrounded both membrane surfaces.

Also no increase of fouling was observed when using WWTP effluents instead of pure water. This can be explained by the negligible concentration of natural organic matter in the wastewater compared to the photocatalyst also present in the feed. Therefore, the contribution of organic fouling to the overall membrane filtration resistance was considered as insignificant.

As it was known that a catalyst cake layer at low CFV was formed on the membrane surface during PMR operation, experiments performed using PhACs have shown that this «second dynamic filtration barrier» was totally ineffective to retain PhACs, although the membrane selectivity towards small organic compounds (i.e. dextran) was improved.

Long-run experiments over a 150h period were performed to assess the membrane separation properties of the Al_2O_3/ZrO_2 ceramic membrane by operating at CFV of 6 m/s. The study's findings were that alumina and titania membranes did not suffer from separation layer damage due to the scraping by photocatalyst particles as the Dex150 rejection of the membrane was preserved in time. Indeed, no significant changes of dextran rejection by Al_2O_3/ZrO_2 100kDa membrane was observed after 150h of experiment. This showed that the membrane permeability was also stable along the 150h trials, which was further evidenced by the stability of the intrinsic membrane resistance to water flux. These findings are consistent with the observations made by *Mozia et al.* [9] and *Szymanksi et al.* [10] in the same experimental conditions.

Perspectives for future research

The results obtained in this study allowed for important insights that will help guide future experiments regarding the operating conditions in which the tests should be performed :

First of all, for future experiments it is advised to have more accurate technical data regarding the pore distribution of the membranes as well as the particle size distribution of the photocatalyst and dextran in order to better apprehend their rejection by size-exclusion. The size distribution of the particles could be measured by using a Laser Diffraction Particle Size Distribution analyser [55] and the membrane porometry via a liquid-liquid displacement method as proposed by Wen Li et al. [56].

Following on from the results obtained for the first research question concerning the conditions which promote fouling, future experiments should be operated at cross-flow velocities prevailing turbulent flow conditions to avoid membranes to be fouled: CFV $\geq$ 6 m/s for MF membranes and CFV $\geq$ 3 m/s for UF.

Additionally, as no significant change in membrane permeability was observed when operating with titania or alumina membranes, future investigations should focus on only alumina membrane material when membrane fouling is the core of the study. Indeed, titania membranes are ten times more expensive compared to alumina ones (i.e. 18€ vs 180€).

Thereafter, to further pursue the investigations regarding fouling mechanisms happening during PMR operation and thereby improving the membrane filtration efficiency, several suggestions can be made :

In order to confirm and quantify the presence of a cake layer, the presence of photocatalyst in the pores as well as the morphology of the TiO_2 particles causing the fouling, one would suggest to further cut/open the membrane(s) and analyse its surface by means of SEM and liquid-liquid porometry method as final steps of the experiment. SEM analysis is quite complex and requires some level of expertise to prepare the samples, although the information obtained would be of great help to step forward.

As ultrafiltration membranes have shown total inability to retain the drugs investigated in this study because of the filtration effects—the molecular sizes of the compounds selected are at least a factor of 100 smaller than the pore size of the membranes, future experiments with this type of membranes should only focus on retaining the photocatalyst. Besides, the filtration of nanoscopic pharmaceuticals should be studied using ceramic nanofiltration (NF) membranes.

Following on from the findings for long-term operation, the analysis of the membrane degradation over a longer time period (e.g. 300h, 400h, 500h, ...) would be suggested to see how far the separation efficiency of the membrane can withstand mechanical abrasion. According to literature [10], the membrane stability was reduced after 400h of PMR operation, although the time at which this decline started is still not well defined.

Therefore, for future developments, the same procedure as for RQ3 should be followed over a longer time period and increase the operating time range until the rejection starts to drop.

Moreover, an analysis of the scoured membrane surface morphology should be performed, using atomic force microscopy (AFM) and/or laser scanning microscopy (LSM), as suggested by Mozia et al. [9]. This analysis would provide further insights into three-dimensional morphological characteristics of the membrane surface in order to assess the potential damage caused over that long-term operating period.

Finally, an economical analysis considering all operating (i.e. energy consumption of the pump) and investment (i.e. membrane, cleaning agents) costs for the membrane filtration part of the PMR system could be performed. Together with the economical analysis of the photocatalytic process already done in the master thesis of Maël Makoudi, an economical evaluation of the whole PMR process could be achieved and thereby assess the economical feasibility of this treatment process at larger scale. Additionally, environmental costs (waste management) could be considered by performing a life cycle assessment of the process and eventually further investigate ways to reduce its environmental impact.

Bibliography

[1] N. Serpone, Y. M. Artemev, V. K. Ryabchuk, A.V. Emeline, and S. Horikoshi. Light-driven advanced oxidation processes in the disposal of emerging pharmaceutical contaminants in aqueous media: A brief review. *Curr. Opin. Green Sustain. Chem.*, 6:18–33, 2017.

[2] W. Zhang, L. Ding, J. Luo, M. Y. Jaffrin, and B. Tang. Membrane fouling in photocatalytic membrane reactors (PMRs) for water and wastewater treatment: A critical review. *Chem. Eng. J.*, 302:446–458, 2016.

[3] Mantec Technical Ceramics. Star-sep. advanced filtration technology. ceramic crossflow membranes. http://www.mantectechnicalceramics.com/sites/default/files/star_sep_brochure.pdf, 2012. [Accessed 16/05/2018].

[4] S. Mozia, A. W. Morawski, R. Molinari, L. Palmisano, and V. Loddo. *Photocatalytic membrane reactors: Fundamentals, membrane materials and operational issues*, volume 2. Woodhead Publishing Limited, 2013.

[5] A. Basile, A. Cassano, and N. K. Rastogi. *Advances in membrane technologies for water treatment : materials, processes and applications*.

[6] E. Abbasi-garravand. Removal of Cr (VI) and Cr (III) From Water by Reduction and Micellar Enhanced Ultrafiltration Techniques. *Sep. Purif. Technol.*, 132(December):505–512, 2012.

[7] D.A. Verona, A. Semião, and B. Antizar-Ladislao. Harvesting microalgae with ultrafiltration membranes. https://sites.google.com/site/algaeultrafiltration/current-issues/fouling-and-flux-optimisation, 2013. [Accessed 04/05/2018].

[8] P. Wang, Anthony G. Fane, and T. T. Lim. Evaluation of a submerged membrane vis-LED photoreactor (sMPR) for carbamazepine degradation and TiO2separation. *Chem. Eng. J.*, 215-216:240–251, 2013.

[9] S. Mozia, K. Szymański, B. Michalkiewicz, B. Tryba, M. Toyoda, and A. W. Morawski. Effect of process parameters on fouling and stability of MF/UF TiO2membranes in a photocatalytic membrane reactor. *Sep. Purif. Technol.*, 142:137–148, 2015.

[10] K. Szymański, A.W. Morawski, and S. Mozia. Humic acids removal in a photocatalytic membrane reactor with a ceramic UF membrane. *Chem. Eng. J.*, 305:19–27, 2016.

[11] Hach Company®. DR/4000 UV-vis Spectrophotometer. https://www.hach.com/dr-4000-u-spectrophotometer-115-vac/product?id=7640447364, 2004. [Accessed 17/05/2018].

[12] Agilent Technologies. *Agilent 1200 Infinity Series Universal Interface Box*. 08/2013 edition, 2013.

[13] Agilent Technologies. Open access lc/ms. https://www.agilent.com/cs/library/brochures/Walkup-LCMS_final_WEB.pdf, 2017. [Accessed 13/05/2018].

[14] P. Walzel. Ullmann's Encyclopedia of Industrial Chemistry. *Ullmann's Encycl. Ind. Chem.*, 14:677–709, 2012.

[15] C. Boillot. Évaluation Des Risques Écotoxicologiques Liés Aux Rejets D'Effluents Hospitaliers Dans Les Milieux Aquatiques. *Recherche*, page 267, 2008.

[16] R Molinari, a Caruso, and L Palmisano. *Photocatalytic Processes in Membrane Reactors*. Number December. 2010.

[17] Y. Pesqueux. La station d'epuration de la Vallee de la Dyle. Technical report, Court-St-Etienne.

[18] J.P. Besse, J.F. Latour, and J. Garric. Anticancer drugs in surface waters. What can we say about the occurrence and environmental significance of cytotoxic, cytostatic and endocrine therapy drugs? *Environ. Int.*, 39(1):73–86, 2012.

[19] A. Eitel, M. Scherrer, and K. Kümmerer. Handling cytostatic drugs : A practical guide. http://www.escoglobal.com/resources/pdf/zyto20_e.pdf, 2000. [Accessed 10/05/2018].

[20] M. Francis. Schistosomiasis. In *Parasit. Dis. - Schistosomiasis*, chapter 4. InTech, jan 2013.

[21] A. Olalla, N. Negreira, M. López de Alda, D. Barceló, and Y. Valcárcel. A case study to identify priority cytostatic contaminants in hospital effluents. *Chemosphere*, 190:417–430, 2018.

[22] International Diabetes Federation. Country summary table: estimates 2017. 2017.

[23] M. Hall, D. Hill, and G. Pave. Global Pharmaceuticals 2016 industry statistics. *Hardman Co Res. Ltd.*, (March):1–16, 2017.

[24] Creative-Biolabs. Cancer Drug R&D and Market Trends from 2006 to 2017. https://www.creative-biolabs.com/blog/index.php/cancer-drug-rd-and-market-trends/, 2018. [Accessed 20/03/2018].

[25] M. Taheran, S. K. Brar, M. Verma, R. Y. Surampalli, T. C. Zhang, and J. R. Valero. Membrane processes for removal of pharmaceutically active compounds (PhACs) from water and wastewaters. *Sci. Total Environ.*, 547:60–77, 2016.

[26] R. Molinari, C. Lavorato, and P. Argurio. Recent progress of photocatalytic membrane reactors in water treatment and in synthesis of organic compounds. A review. *Catal. Today*, 281:144–164, 2017.

[27] U. Von Gunten. Particle Removal for wastewater treatment. Technical report, EPFL, Lausanne.

[28] U. Von Gunten. Oxidation and Disinfection Processes in Water Treatment. Technical report, EPFL, Lausanne.

[29] C. Comninellis, A. Kapalka, S. Malato, S. A Parsons, I. Poulios, and D. Mantzavinos. Advanced oxidation processes for water treatment: advances and trends for R&D. *J. Chem. Technol. Biotechnol.*, 83(6):769–776, 2008.

[30] L. Ferrando-Climent, S. Rodriguez-Mozaz, and D. Barceló. Incidence of anticancer drugs in an aquatic urban system: From hospital effluents through urban wastewater to natural environment. *Environ. Pollut.*, 193:216–223, 2014.

[31] J. Zhang, V.W. C. Chang, A. Giannis, and J. Y. Wang. Removal of cytostatic drugs from aquatic environment: A review. *Sci. Total Environ.*, 445-446:281–298, 2013.

[32] S. Mozia. Photocatalytic membrane reactors (PMRs) in water and wastewater treatment. A review. *Sep. Purif. Technol.*, 73(2):71–91, 2010.

[33] X. Zheng, Z. P. Shen, L. Shi, R. Cheng, and D.-H. Yuan. Photocatalytic Membrane Reactors (PMRs) in Water Treatment: Configurations and Influencing Factors. *Catalysts*, 7(8):224, 2017.

[34] S. Mozia, A. W. Morawski, M. Toyoda, and M. Inagaki. Effectiveness of photodecomposition of an azo dye on a novel anatase-phase TiO2 and two commercial photocatalysts in a photocatalytic membrane reactor (PMR). *Sep. Purif. Technol.*, 63(2):386–391, 2008.

[35] G. Tchobanoglous, J.C. Crittenden, K.J. Howe, R.R. Trussell, and W.H. David. *MWH's Water Treatment: Principles and Design...* John Wiley & Sons, 3rd edition, 2012.

[36] E. Hoek. MF/UF Membrane Filtration: A State-of-the-Art Review.

[37] X. Shi, G. Tal, N. P. Hankins, and V. Gitis. Fouling and cleaning of ultrafiltration membranes: A review. *J. Water Process Eng.*, 1:121–138, 2014.

[38] M.J. Akers, C. S. Strother, and M. R. Walden. *Fermentation and Biochemical Engineering Handbook*. 1996.

[39] S. O. Ganiyu, E. D. Van Hullebusch, M. Cretin, G. Esposito, and M. A. Oturan. Coupling of membrane filtration and advanced oxidation processes for removal of pharmaceutical residues: A critical review. *Sep. Purif. Technol.*, 156:891–914, 2015.

[40] A. J. C. Semião and A. I. Schäfer. Xenobiotics Removal by Membrane Technology: An Overview. pages 307–338, 2010.

[41] R. Janssens, M. K. Mandal, K. K. Dubey, and P. Luis. Slurry photocatalytic membrane reactor technology for removal of pharmaceutical compounds from wastewater: Towards cytostatic drug elimination. *Sci. Total Environ.*, 599-600(2017):612–626, 2017.

[42] J. Garcia-Ivars, J. Durá-María, C. Moscardó-Carreño, C. Carbonell-Alcaina, M. I. Alcaina-Miranda, and M. I. Iborra-Clar. Rejection of trace pharmaceutically active compounds present in municipal wastewaters using ceramic fine ultrafiltration membranes: Effect of feed solution pH and fouling phenomena. *Sep. Purif. Technol.*, 175:58–71, 2017.

[43] S. J. Lee, M. Dilaver, P. K. Park, and J. H. Kim. Comparative analysis of fouling characteristics of ceramic and polymeric microfiltration membranes using filtration models. *J. Memb. Sci.*, 432:97–105, 2013.

[44] H. Choi, K. Zhang, D. D. Dionysiou, D. B. Oerther, and G. A. Sorial. Effect of permeate flux and tangential flow on membrane fouling for wastewater treatment. *Sep. Purif. Technol.*, 45(1):68–78, 2005.

[45] E. Zuriaga-Agustí, E. Alventosa-deLara, S. Barredo-Damas, M. I. Alcaina-Miranda, M. I. Iborra-Clar, and J. A. Mendoza-Roca. Performance of ceramic ultrafiltration membranes and fouling behavior of a dye-polysaccharide binary system. *Water Res.*, 54:199–210, 2014.

[46] TAMI Inudustries. Technical Directions for 25-60-120 Housings. http://www.tami-industries.com/enadvanced-ceramic-filtration/, 2004. [Accessed 20/04/2018].

[47] H. Wahid, S. Ahmad, M.A.M. Nor, and M. A. Rashid. Material Safety Data Sheet. *Econ. J. Malaysia*, 51(2):39–54, 2017.

[48] E. Theodorsson. Limit of detection , limit of quantification and limit of blank LoB , LoD , LoQ. *Talanta*, 129:606–616, 2014.

[49] M. A. Anderson, M. J. Gieselmann, and Q. Xu. Titania and alumina ceramic membranes. *J. Memb. Sci.*, 39(3):243–258, 1988.

[50] H. Jiang, L. Meng, R. Chen, W. Jin, W. Xing, and N. Xu. Progress on porous ceramic membrane reactors for heterogeneous catalysis over ultrafine and nano-sized catalysts. *Chinese J. Chem. Eng.*, 21(2):205–215, 2013.

[51] F. Russo and N.T. Basse. Scaling of turbulence intensity for low-speed flow in smooth pipes. *Flow Meas. Instrum.*, 52(October):101–114, 2016.

[52] M. Bahrami. Fluid Mechanics (S 09). Viscous Flow in Ducts. http://www.sfu.ca/ mbahrami/ENSC 283/Notes/Viscous Flow in Ducts.pdf, 2009. [Accessed 28/05/2018].

[53] L. Song, B. Zhu, S. Gray, M. Duke, and S. Muthukumaran. Hybrid processes combining photocatalysis and ceramic membrane filtration for degradation of humic acids in saline water. *Membranes (Basel).*, 6(1), 2016.

[54] H. K. Shon, S. Vigneswaran, J. Kandasamy, and J. Cho. Characteristics of Effluent Organic Matter in Wastewater. *UNESCO - Encycl. life Support Syst. Water wastewater Treat. Technol.*, (January):1–17, 2007.

[55] A. Mendoza, J. Aceña, S. Pérez, M. López de Alda, D. Barceló, A. Gil, and Y. Valcárcel. Pharmaceuticals and iodinated contrast media in a hospital wastewater: A case study to analyse their presence and characterise their environmental risk and hazard. *Environ. Res.*, 140:225–241, 2015.

[56] W. Li, G. Ling, F. Lei, N. Li, W. Peng, K. Li, H. Lu, F. Hang, and Y. Zhang. Ceramic membrane fouling and cleaning during ultrafiltration of limed sugarcane juice. *Sep. Purif. Technol.*, 190(August 2017):9–24, 2018.

[57] I. Kim and H. Tanaka. Photodegradation characteristics of PPCPs in water with UV treatment. *Environ. Int.*, 35(5):793–802, 2009.

Appendices

Appendix A : Photocatalysis

Photocatalysis is termed as a 'Green process' as it helps reducing the use and generation of toxic substances along with a human-health and environmental risk. Several green characteristics of photocatalysis can be outlined such as operating under mild conditions (near room temperature and pressure), abatement of contaminants while mitigating generation of harmful byproducts and use of (chemically) stable photocatalyst(s) (e.g. TiO_2).

A.1 Photocatalysts

The ideal photocatalyst must match the following criteria : suitable bandgap energy, chemical and physical stability, available, nontoxic nature and low cost. Many materials match these latter criteria and among these, the most widely used is a nanosized titanium oxide combination as it is the case for *Degussa P25* [16]. Degussa P25 is composed of 20% rutile titania, which is the most stable crystalline structure with respect to anatase and brookite, and 80% anatase titania which has the highest reduction power [34]. Titania matches not only advantageous intrinsic electronic properties but also surface physico-chemical and morphological ones. Indeed, nanoparticles due to their quantum size effect and high surface area, achieve high photoactivity and selectivity [16]. Altogether, these features spotlight TiO_2 as the most appealing photocatalyst as being chemically stable, low-cost, non-toxic and abundant on the market.

A.2 Light source

These wavelengths (387 and 380 nm) match the UV spectrum range. Nowadays, the lamps most commonly used are the low- and high-pressure mercury lamps (LP and MP). The LP lamp, irradiating at lower wavelength (around 254nm) has shown to be more efficient for degrading some pharmaceuticals [57] as more energetic photons are emitted. Furthermore, the increasing light intensity enhances the photocatalytic reaction under a certain threshold value.

Indeed, up to date, the polymorphous titania (anatase, rutile and brookite) band gap(s) only absorbs radiations with wavelengths lower than $\pm$400nm, corresponding $\pm$5% of visible light [4]. Sunlight harvesting allows to avoid high costs of the light sources used nowadays (low and high pressure UV lamps, mercury lamps, LEDs, ...). Higher intensity lamps such as light-emitting diodes (LEDs) [8], additionally to their higher degrading power, also avoid mercury disposal problem and show their lifetime extended [41].

In the photocatalytic process, TiO_2 catalyzes redox reactions generating hydroxyl radicals ($OH^{\bullet}$) which further oxidize with some sundry scavengers present in the water as presented in the following section. These previously unique PMR characteristics aim at improving the efficiency and stability of the process along with reducing the operating costs by regeneration of the catalyst.

A.3 Photodegradation mechanism

The way how these photocatalytic-material and UV-light interact together to finally degrade the pollutants is now presented.

Semiconductors are used to perform this catalysis-task because once they are excited by high-energy photons ($E_{photon} \geqq E_{bandgap}$), an electron is promoted from the valance band (VB) to the conduction band (CB) leaving a hole behind (electron-hole pair created). Each of these subatomic particles give rise to redox reactions: either an oxidation reaction (holes) or either a reduction one (electron).

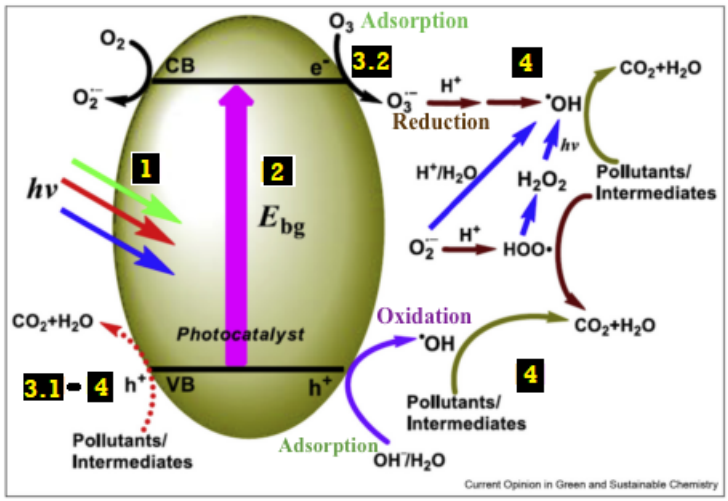

Figure A.1: Photocatalytic mechanisms taking place in UV/visible light-irradiated photocatalyst [1]

1. Photoactivation step [1]: $\boxed{TiO_2 + \text{h}\nu \rightarrow TiO_2(e^- + h^+)}$
2. Step [2] includes the charge separation followed by either an electron-hole pair recombination or a charge transfer towards the catalyst surface
3. Step [3.1] either the excited charge interacts directly with the organic contaminant (direct mineralization) $\Rightarrow Step[4]$
4. Step [3.2] or the excited charges interect by intermediacy of reactive oxidants (O_2, O_3, OH^- or H_2O) hence generating radicals/superoxide species
5. Step [4] consists of the final degradation (partial and/or complete) through direct/intermediate photocatalytic redox reactions [26]:

Appendix B : Fouling control strategies

1. **Self-cleaning process** (by photocatalytic oxidation) : degradation of organic pollutants $\Rightarrow$ less foulants

2. **Feed pretreatment** : optimisation of foulant-foulant and/or foulants-membrane interactions by addition of a coagulant and pH adjustments

3. **membrane modification** : enhancement of the hydrophilicity and antifouling ability by implantation of polar organic functional groups onto membrane surface [2].

4. Apply **aeration** at optimal rate of 0.5 L/min (according to [2]) or **intermittent permeation** providing in both cases some turbulence on the membrane surface resulting in a reduction of catalyst deposition along with keeping this latter well suspended in the solution

5. Applied **electric field** as used in photo-electrocatalytic membrane reactors by endowing the membrane with photo-electrocatalytic function by means of a $TiO_2/carbon/Al_2O_3$ anode [8].

6. **Optimization of operating parameters** : optimal range of temperature, cross-flow velocity and permeate flux help reducing the fouling severity. Especially filtration at a critical permeate flux (low flux behavior), following the "critical flux" concept developed by Field et al., showed almost no flux decline and absence of irreversible fouling, although productivity is called into question [2].

7. **Membrane cleaning** : physical and chemical cleaning are fouling removal mechanisms towards which a lot of attention has been drawn for the past decade in order to find an ideal combination of the two which would maximize fouling removal and minimize the high operating cost(s) (mostly associated with the chemicals used) [2].

Appendix C : Experimental starting procedure

Before starting a new experiment, a starting procedure was followed in order to get rid of all the air present in the closed reactor-membrane system in order for the feed-flux sensor to work properly. Indeed, the flux detector operates by means of ultrasonic waves to determine the feed cross-flow velocity. When air bubbles circulate in the system, they interfere with these waves and therefore distort the flow measurement, making this detector useless.

N°	Steps	Cumulative operation time
1	Fill the reactor with 1,6 L of water	1 min
2	Launch the pump by opening the pressure plug valve	2 min
3	Fully open the system valve and set the operating pressure at 0,5 MPa	5 min.
4	Almost close the pressure plug valve to reach very low pressure conditions (< 0,1 bar on monitor)	9 min.
5	Fully open the pressure valve and almost close the system valve	12 min.
6	Degasification : Fully reopen the system valve and go back to low-pressure conditions	16 min.
7	Close the system valve and fully reopen the pressure valve	/
8	Progressively opening of the system valve till the desired cross-flow velocity and pressure have been reached	/

Table C.1: Startup procedure

Appendix D : Calibration curves

Calibration curves have been established for each model compound (Dextran or TiO_2) used to relate the analytical information provided by a specific method (Area for ELSD and Absorbance for spectrophotometer) to the associated concentration value of the sample (feed or permeate).

D.1 Calibration curve for Dextran 110kDa

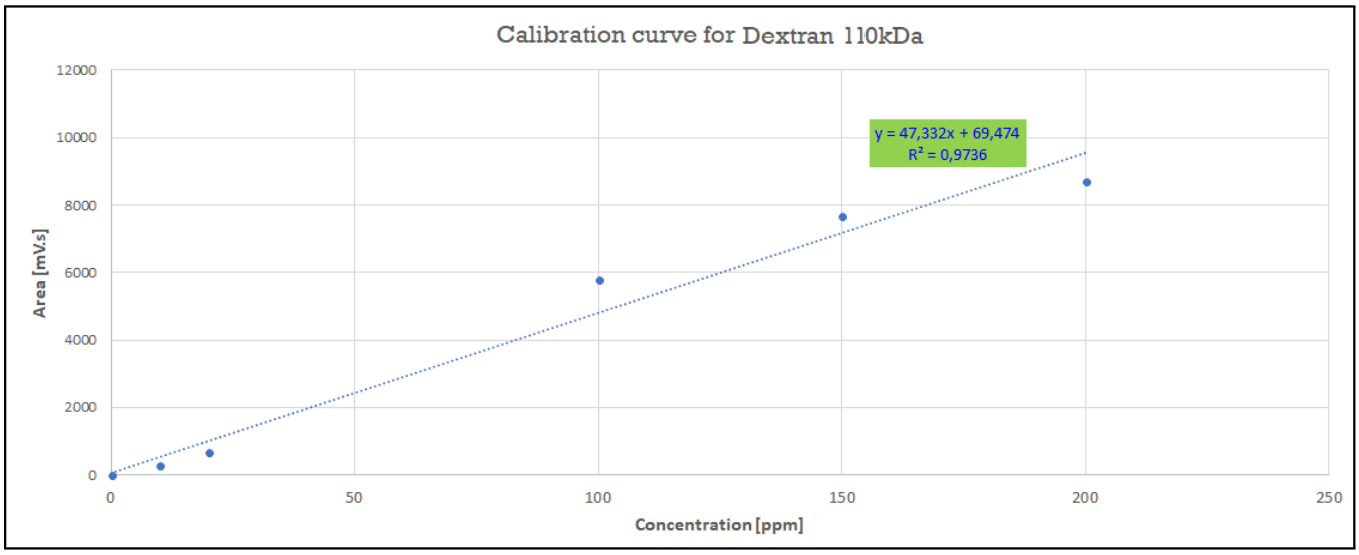

Figure D.1: Calibration curve for Dextran 110kDa by ELSD

D.2 Calibration curve for Dextran 150kDa

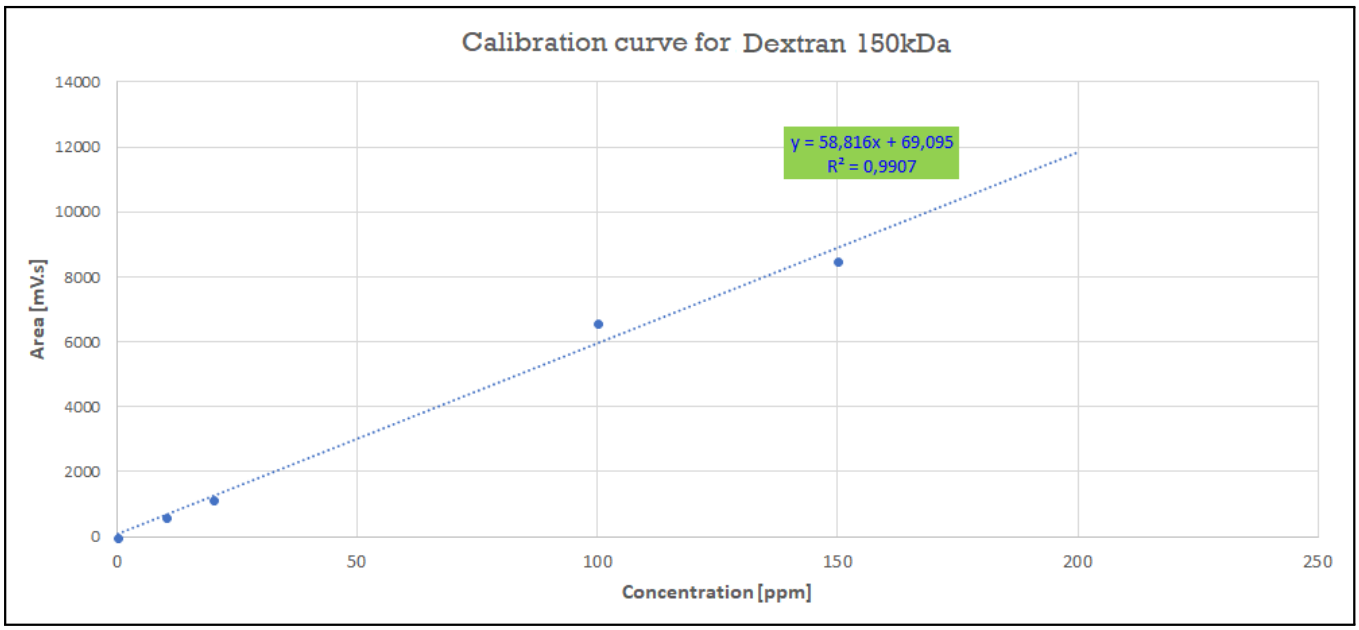

Figure D.2: Calibration curve for Dextran 150kDa by ELSD

D.3 Calibration curve for P25 TiO_2

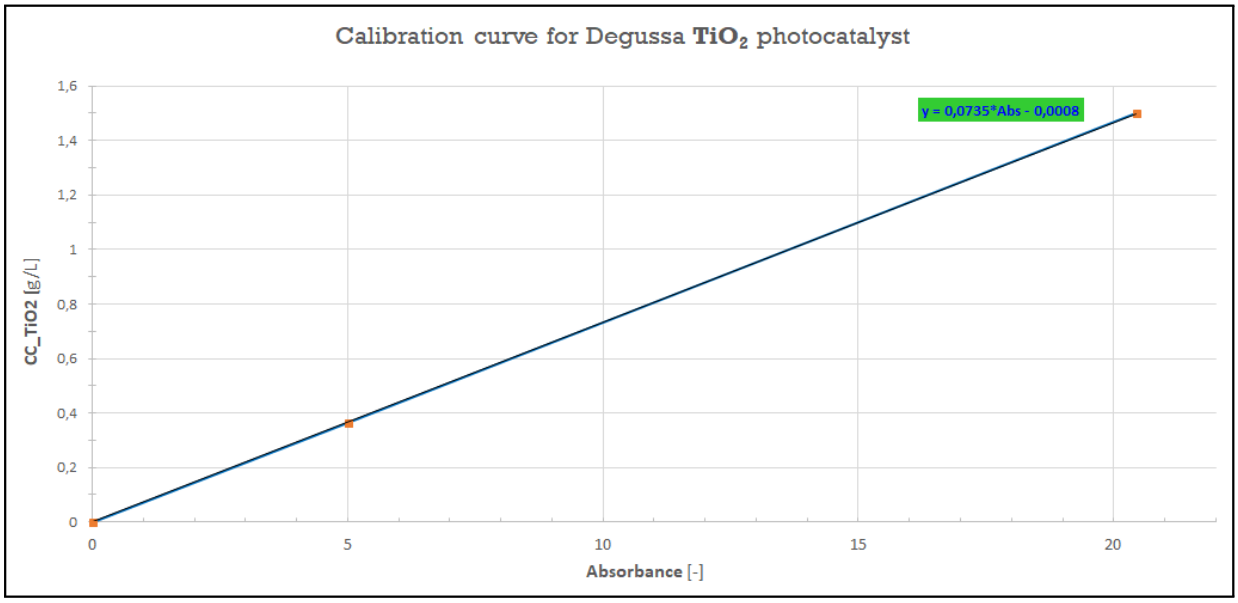

Figure D.3: Calibration curve for Degussa Aeroxide® P25 TiO_2 by spectrophotometer

Appendix E : Additional Results

E.1 Cleaning procedures

At the end of each experiment, the membrane had to be cleaned and therefore an effective cleaning procedure to remove the irreversible fouling matter left on the membrane surface and into the pores had to be found. For this procedure to be effective it should reinitialise the membrane permeability to its initial pure water value measured at the beginning of the experiment. After several combination trials, as shown on Fig. E.1, the following effective method was found :

1. **T°** : First, the membrane was put in the oven at 250°C for 2h in order to burn the organic particles left in the pores
2. **US** : Then it was placed in an ultrasonic bath for 20 minutes to break the aggregated catalyst particles and further degrade organic compounds trapped into the small pores
3. **A/B** : Finally, chemical cleaning by using successively NaOH and H_3PO_4 to respectively perform an alkaline and acidic cleaning in order to remove the remaining organic and inorganic deposits.

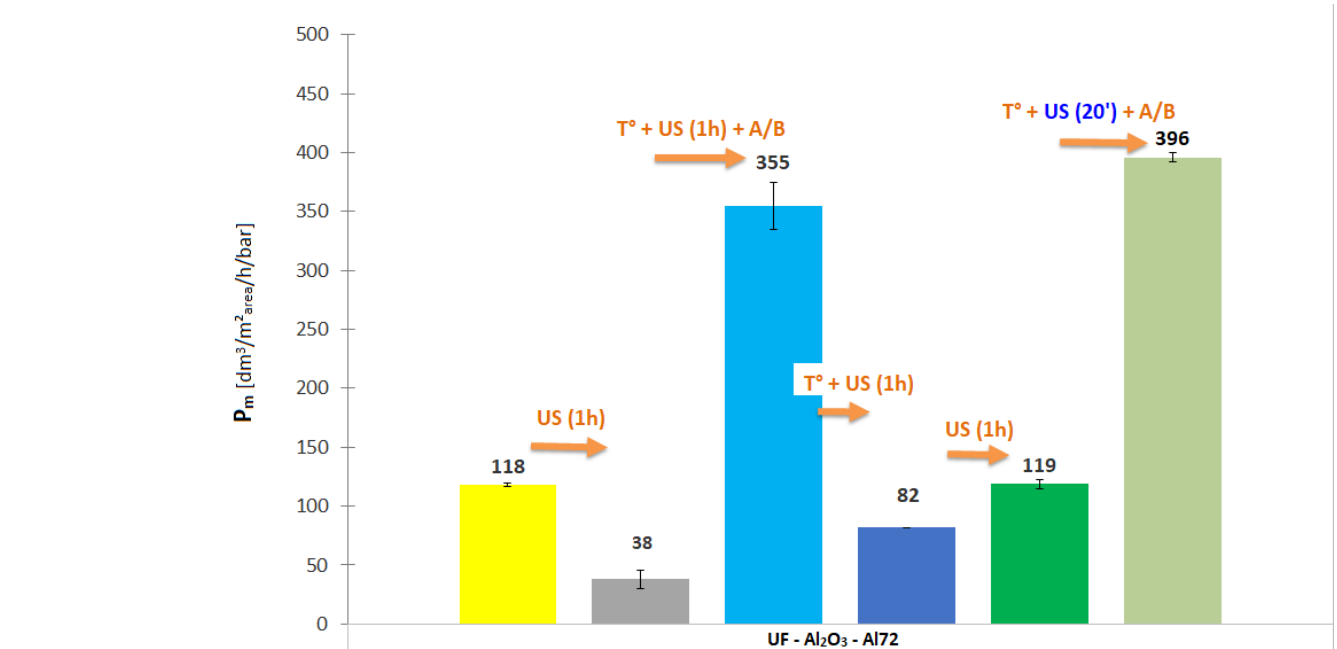

Reference	118
Clean US (10')	38
Clean T° (250°C - 2h), A/B and US (1h)	355
Cleant T° (250°C - 2h) + US (1h)	82
Clean US (1h)	119
Clean T°(250°C - 2h) + US (20') + A/B	396

Figure E.1: Permeability improvement by applying different cleaning procedures for 1 channel alumina (Al72) UF (100kDa) membrane (process paramters : TMP = 3 bar, CFV = 3 m/s, 1g/L Dex110)

E.2 Membrane rejection of dextran 110 kDa

The first probe compound which was initially selected to evaluate the membrane rejection was dextran with a molecular weight of 110 kDa which is slightly higher compared to MWCO of the UF (100kDa) membranes under investigation. Therefore, it was expected that this sugar would be well-retained by these membranes which was also confirmed by the findings of Mozia et al. [9] who found rejection values up to 99% in the same operating conditions as the one used in this work. However, in this study the rejection performance of the UF membranes was almost superfluous as shown in Fig. E.2. This could be explained by the wide pore size distribution of the ceramic membranes.

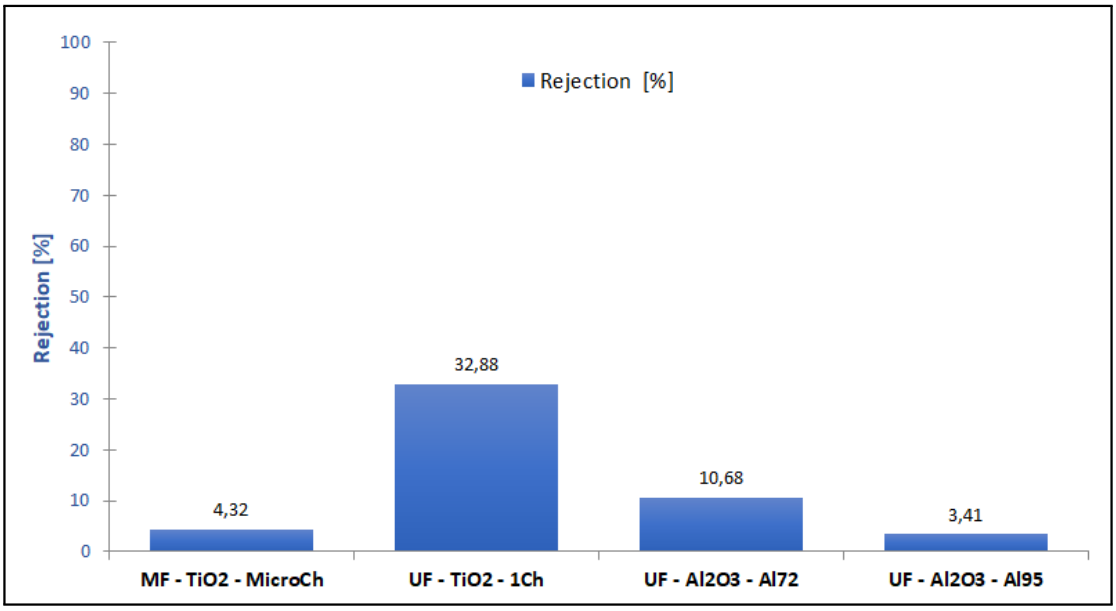

Figure E.2: Membrane rejection of dextran 110 kg/mol (process paramters : TMP = 3 bar, CFV = 3 m/s, 1g/L Dex110)

E.3 Influence of higher turbulent conditions (pulse dampener OFF/ON)

In order to evaluate the impact of the flow turbulence on the membrane permeability, the pulse dampener was alternately switched OFF and ON and thereby promoting (high) turbulence in the feed flow. However, the results shown in Fig. E.3 do not evidence a change in the membrane permeability for higher turbulent flow conditions.

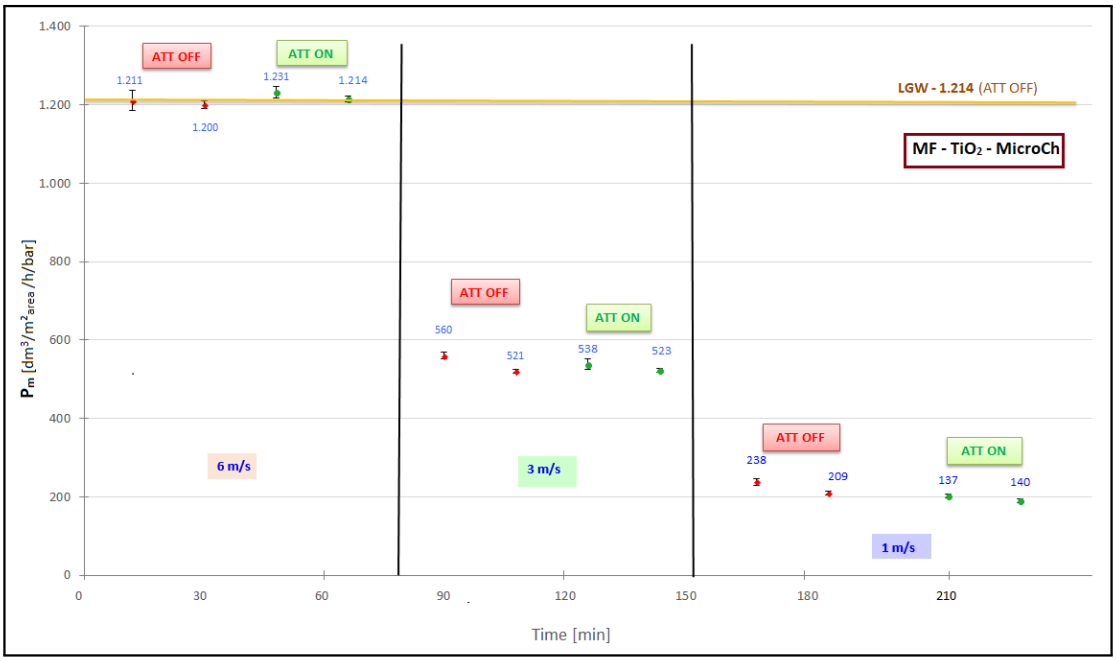

Figure E.3: Influence of pulse attenuator on membrane permeability of 1 channel TiO_2 MF(0,2μm) membrane (process paramters : TMP = 3 bar, 1.5 g/L TiO_2, CFV = 6, 3 and 1 m/s)

Rue Archimède, 1 bte L6.11.01, 1348 Louvain-la-Neuve **www.uclouvain.be/epl**